The Pennsylvania State University

The Graduate School

APPLICATIONS IN SUPRAMOLECULAR CHEMISTRY: POLYMER BASED ANION RECOGNITION AND POLYMORPH MODIFICATION

A Thesis in

Chemistry

by

Tanner Geibel

Submitted in Partial Fulfillment
of the Requirements
for the Degree of

Master of Science

August 2020

The thesis of Tanner Geibel was reviewed and approved by the following:

Elizabeth Elacqua
Assistant Professor of Chemistry
Thesis Advisor

Paul Cremer
J. Lloyd Huck Professor of Chemistry
Professor of Biochemistry and Molecular Biology

Michael Hickner
Professor of Materials Science and Engineering
Professor of Chemical Engineering
Professor of Chemistry

Robert Hickey
Assistant Professor of Materials Science and Engineering

Phil Bevilacqua
Distinguished Professor of Chemistry
Professor of Biochemistry and Molecular Biology
Head of the Department of Chemistry

ABSTRACT

The design and modification of supramolecular interactions and self-assembly in synthetic polymers and biopolymers is described. Many synthetic routes were attempted to make a calix[4]pyrrole-chromophore conjugate that was capable of polymer/monomer attachment. A polymer was synthesized bearing calix[4]pyrrole-BODIPY conjugate side chains, which was used for fluoride recognition and capture, affording a colorimetric and fluorometric response. Chemical modifications to cellulose's hydrogen bonding structure with diamines were investigated to convert the natural polymer to different polymorphs. Attempts were made at utilizing this process to align cellulose in an external magnetic and electric field. Current work is being conducted to better understand the kinetics of the conversion between cellulose polymorphs.

TABLE OF CONTENTS

LIST OF FIGURES

LIST OF TABLES

LIST OF SCHEMES

ACKNOWLEDGEMENTS

I would like to first thank my advisor Beth Elacqua, who has always been available to provide me with insight into my project and mental support. Her consistent encouragement, answering of my questions, and providing me with constructive feedback has given me the tools needed to succeed as a chemist.

I would also like to thank Paul Cremer, Mike Hickner, and Rob Hickey for being my committee members throughout my time as a graduate student. Thank you for the feedback and encouragement on my projects during my time at Penn State.

I would like to thank the rest of the Elacqua lab, in particular Mitch and Hugo for always being willing to synthesize compounds, regardless of how ridiculous the scale. Additionally, I need to thank Shalisa, Margaret, Steve, Julia, Danny, and Lucas for giving me feedback on my paper and presentation. Also, I have to thank two of my best friends in the Elacqua lab, Stephen and Jake, who have always provided me with constructive criticism on my project. I am looking forward to seeing where the three of us all end up as we go in our new directions.

I would like to thank my collaborators on the collaborative cellulose project. In particular, many thanks go to Inseok from the Kim group and Kassem from the Catchmark group. I would like to acknowledge that work in Chapter 4 was supported by a seed grant (iSuperSEED) from the National Science Foundation under MRSEC Grant No. DMR-1420620. Findings and conclusions do not necessarily reflect the view of the funding agency.

I would finally like to thank my parents for consistent support in all that I do. I would not be where I am today without them. ILYBTTW

Chapter 1

Introduction to Supramolecular Chemistry

In 1993, Jean-Marie Lehn defined supramolecular chemistry as "chemistry beyond the molecule."[1] Supramolecular chemistry is concerned with electrostatic interactions weaker than that of a covalent bond, such as hydrogen bonding, π-π interactions, metal coordination, and host-guest chemistry (Figure 1). As these have been observed to be

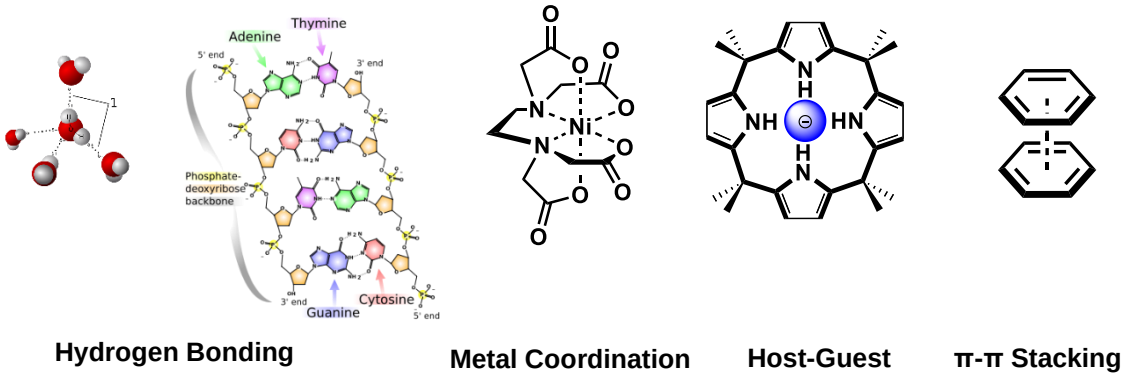

Figure 1. Examples of Supramolecular Interactions

weaker than covalent bonds, these are often also termed noncovalent interactions. Fundamental biological observations are governed by supramolecular chemistry; enzymes bind guest molecules and the DNA double helix is held together by hydrogen bonding and π-π stacking. In 1987, the Nobel prize in chemistry was awarded for work in supramolecular chemistry to three scientists: Jean-Marie Lehn for the synthesis of cryptands, Charles Pedersen for investigating crown ethers, and Donald Cram for work in the field of host-guest chemistry.[2]

Host-guest chemistry is a subsection of supramolecular chemistry where two molecules or ions are held together by noncovalent electrostatic interactions. In this field, a larger host molecule is commonly designed to bind a smaller molecule or anion. This recognition event allows for host molecules to often be used as sensors and extract guests from solution. Hosts are often macrocycles, which are defined as molecules containing at minimum a twelve-membered ring.[3] The most common macrocycles have some degree of symmetry and are easy to synthesize, usually by connecting smaller rings together by a bridge through condensation reactions. These host molecules have been used in many applications, and their functionalization has expanded the utility of host-guest chemistry considerably.

Supramolecular chemistry has been applied in a variety of areas, such as environmental, biological, synthetic, and materials chemistry.[4] Recent studies have focused on the development of supramolecular motifs that have been used extensively to bind and remove both cationic and anionic species which can pose threats to public health.[5,6] Noncovalent interactions have been used to remove small molecule pollutants, such as perfluorooctanoic acid (PFOA) and perfluorooctane sulfonate (PFOS), from water.[7] Supramolecular systems have been used extensively in biology, with one such application being controlled drug delivery.[8,9] Another important application centers on evaluating health of individuals through sensing of specific metabolites and toxins.[10,11,12] In addition, there is a growing utility in methodology development, particularly in catalysis,[13] and this has been used in the total synthesis of natural products.[14] Regarding materials applications, crosslinking polymers through noncovalent interactions has been used extensively, with many designs focused on the development of self-healing

materials[15] that exploit the inherent reversibility of these interactions. A benefit of incorporating supramolecular motifs into materials, particularly polymers, is that they can be used to further aspects of environmental, biological, and synthetic applications. Specifically, polymers can overcome specific challenges in the development of these applications, such as solubility in desired solvents, particularly water, while lending recyclability to certain applications.

Hydrogen Bonding

The hydrogen bond is a specific type of noncovalent interaction, which is governed by strong dipole-dipole interactions. In particular, when hydrogen is bound to a highly electronegative atom, that H-atom becomes electron deficient and is attracted to atoms with high electron density, specifically oxygen, nitrogen, and fluorine. Because of this, many liquids like water and simple alcohols have homo-molecular hydrogen bonding that give rise to their physical properties.

As previously stated, hydrogen bonding plays a very important role in biological interactions. The two helices within DNA are held together by the strong hydrogen bonding interactions of the nucleobases. The secondary structures within proteins are also commonly the result of hydrogen bonding, mostly due to the intramolecular interactions between amides.[16] Another common biomacromolecule, cellulose, has many hydroxy side-chains that hydrogen bond with one another, giving it great mechanical strength and stability.[17]

While prevalent in biological systems, synthetic chemists have developed molecules that also have characteristics derived from hydrogen bonding interactions. For example, a fluorescent napthalimide was synthesized and used as a fluorescent pH sensor due to its formation of an intramolecular hydrogen bond under acidic conditions, leading to fluorescence quenching.[18] Hydrogen bonding has also been used for enantioselective small molecule methodology.[19] Recently, Jacobsen and coworkers used a chiral squaramide as a hydrogen donor to silyl triflates to make a highly activated Lewis acid, which was used as a catalyst for enantioselective alkylation of acetals.[20] Synthetic receptors have also been developed based on their hydrogen bond capabilities. Examples of such receptors are a class of barbiturate binding macrocycles made from two 2,6-diaminopyridines linked together with an isophthalic group (Figure 2).[21] This is an example of how hydrogen bonds can be used efficiently in host-guest chemistry.

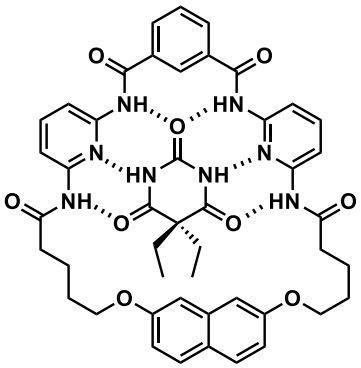

Figure 2. Structure of diaminopyridine receptor binding barbital.

Small-Molecule Host-Guest Chemistry

Small-molecule supramolecular host-guest chemistry has been studied extensively to include molecules such as crown ethers, cryptands, cyclodextrins, calixarenes, pillararenes, cucurbiturils, and many more. Crown ethers are macrocyclic poly(ether)s with

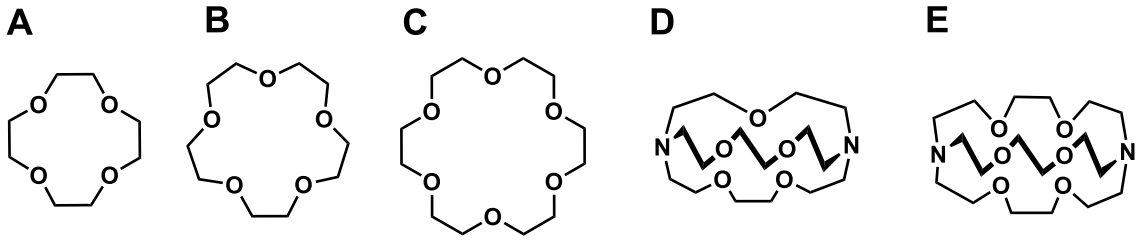

Figure 3. Structures of 12-crown-4 **(A)**, 15-crown-5 **(B),** and 18-crown-6 **(C)** ethers. Structures of 2,2,1-cryptand **(D)** and 2,2,2-cryptand **(E)**.

varying cavity diameter and high affinity for alkali metals such as potassium and lithium (Figure 3 A-C).[22] They are commonly used as phase-transfer catalysts to bring inorganic catalysts such as salts into the organic phase. Cryptands are bicyclic and sometimes polycyclic molecules that have affinity to alkali metals, but are more selective as they are more rigid in nature (Figure 3 D,E).[23] Recently, cryptands have been made using sucrose scaffolds, which has enabled ease of cavity diversification.[24]

Calix[n]arenes are "chalice-like" macrocycles composed of four or more phenol units, where n is equal to the number of phenol units within the ring; the most common of these is *p*-tert-butylcalix[4]arene (Figure 4A).[25] The aromatic ring and hydroxy moieties have been functionalized extensively for a variety of applications. For instance, a boron-dipyrromethane (BODIPY)-bound calixarene was shown to be capable of fluorometrically sensing Ca^{2+} (Figure 3B).[26] Recently, a supramolecular host similar to calixarenes, coined

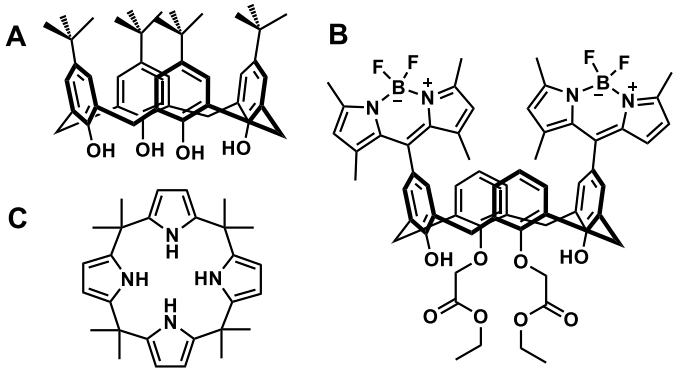

Figure 4. Structures of p-tert-butyl calix[4]arene (**A**) and a BODIPY, calixarene capable of sensing Ca^{2+} (**B**), and meso-octamethyl calix[4]pyrrole (**C**).

a pillararene, was developed from the condensation of multiple hydroquinone units.[27] Calixpyrroles are another class of host molecules which have been used extensively for their anion recognition. The most common of this class of macrocycle is meso-octamethylcalix[4]pyrrole (Figure 4C), which has a strong affinity for fluoride.[28]

Cyclodextrins are cyclic oligosaccharide guest molecules with many biological uses. For instance, water-soluble cyclodextrins have been used as complexing agents for drug delivery of nitroglycerin, omeprazole, and piroxicam.[29] Another class of barrel-shaped macrocycles is cucurbit[n]urils, which are composed of multiple glycoluril units. Cucurbiturils are very rigid, a result of each glycoluril unit having four bridging sites, as opposed to units in other common macrocycles only having two (Figure 5).[30] The rigid hydrophobic cavity of cucurbiturils have made them a great tool for binding nonpolar guest molecules. They have been used to bind neutral species such as tetrahydrofuran or diethyl ether. The polar exteriors of cucurbiturils are good for binding cations, which can act like "lids" to contain neutral species within the nonpolar cavity.[31]

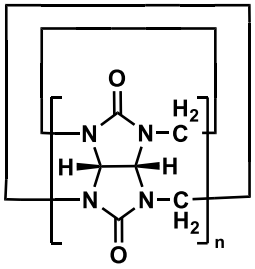

Figure 5. Structure of cucurbiturils.

Host-Guest Chemistry in Polymers

Supramolecular chemistry has been studied extensively in polymer systems as well, often either as pendant groups that participate in noncovalent interactions, or as supramolecular polymers, which are often made from molecules that have a minimum of two interaction sites that coordinate to one another. Crown ethers have been used in the development of both of the aforementioned polymers. There are many examples of crown

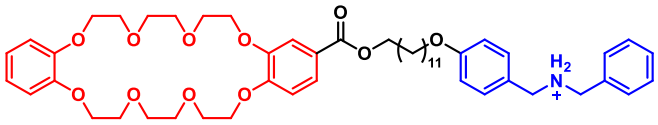

Figure 6. Small molecule which coordinates intermolecularly between crown ether and ammonium salt moieties to form supramolecular polymers.

ethers in polymers,[32] such as the small molecule in Figure 6, which contains both a crown ether (host) and an ammonium salt (guest) with high affinities for one another, allowing it form a gel under ambient conditions.[33] Crown ethers have also been incorporated into polymers as pendants. For example, a poly(phenylacetylene) bearing a crown ether side-chain has been used to bind amino acids (Figure 7A).[34] When binding specific isomers of amino acids, the polymer formed a helix and could be characterized by circular dichroism (CD). Different handed helices formed depending on the chirality of the amino acid used, so they could use CD to determine the absolute configuration of the amino acids present in a solution of this crown ether containing polymer. Recently a pseudo cryptand-containing copolymer was developed that could be used to selectively sense Al(III).[35]

Calixarenes have been used extensively in polymers as well. Pendant calixarenes have been incorporated into copolymers with methyl acrylate, acrylonitrile, and styrene

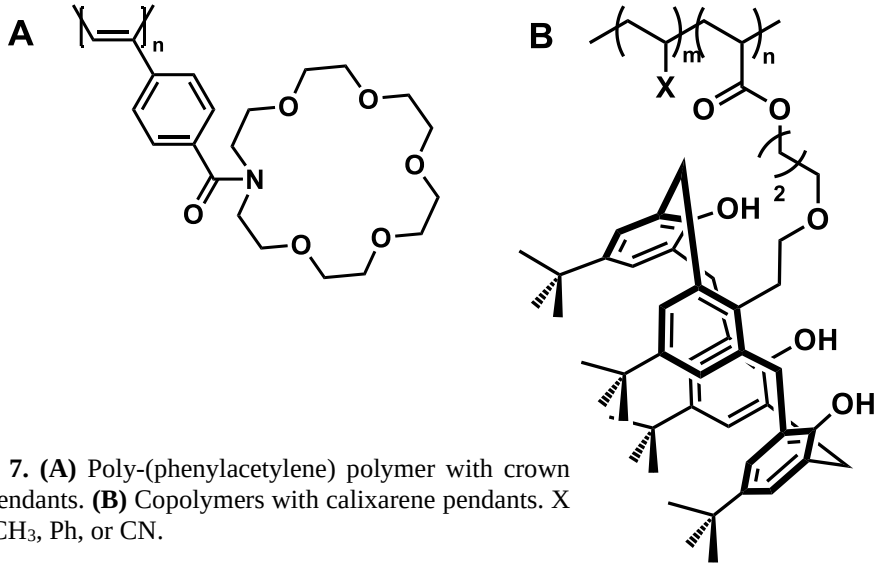

Figure 7. (A) Poly-(phenylacetylene) polymer with crown ether pendants. **(B)** Copolymers with calixarene pendants. X = CO_2CH_3, Ph, or CN.

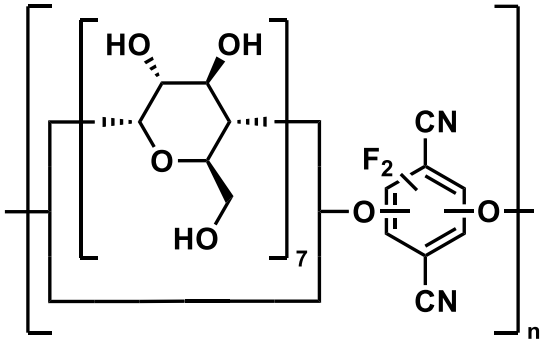

Figure 8. Polymer made up of β-cyclodextrin units used for removal of micropollutants.

backbones (Figure 7B).[36] Homopolymers with calixarene side-chains have been made as well, which were used to complex with sodium ions in solution.[37] Cyclodextrins have also found many uses in polymers as macrocycles that could be used to remove dyes[38] and heavy metals such as Pb(II), Cd(II), and Ni(II)[39] from aqueous systems. A more recent example of the utility of cyclodextrin-based polymers came in 2016 when Dichtel and coworkers made a porous β-cyclodextrin-based polymer (Figure 8) that was capable of removing micropollutants from aqueous systems such as bisphenols, metolachlor, propranolol, and ethinyl oestradiol.[40]

Supramolecular Interactions in Synthetic Polymers

Hydrogen bonding in polymers has been extensively studied. For instance, Meijer and coworkers have made supramolecular polymeric materials that arise from hydrogen bonding of ureidopyrimidone units (Figure 9).[41] Hydrogen bonding has also been used in the development of poly(ether-thioureas) that can heal following fractures through compression at ambient temperatures.[42] Pi stacking is another supramolecular interaction that has found use in synthetic polymers, as recently Weck and coworkers were able to design polymers with β-sheets.[43] They were able to achieve this through

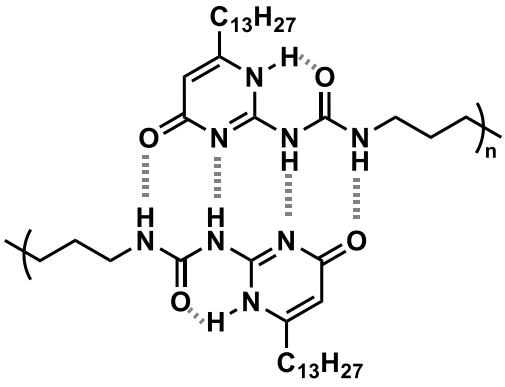

Figure 9. Supramolecular polymer from hydrogen bonding of ureido-pyrimidone units.

the use of phenyl / perfluorophenyl interactions to induce turns that allowed for pi stacking interactions of poly(p-phenylenevinylene) chains, effectively making β-sheet type interactions.

Thesis Overview

All of the aforementioned functional polymeric materials displayed versatile applicability due to the integration of supramolecular motifs. The focus of this thesis will be on two different supramolecular interactions in polymeric systems, host-guest based anion recognition and hydrogen bonding. The host-guest systems discussed above integrated a variety of macrocycles that could participate in some level of molecular recognition. Chapter 2 focuses on small-molecule synthetic routes to develop a colorimetric anion sensor based on a calix[4]pyrrole-based host. Chapter 3 introduces a new synthetic route that was successful in attaching a calix[4]pyrrole-based colorimetric anion sensor to a polymer. Chapter 4 discusses how hydrogen bonding interactions within cellulose can be disrupted by primary amines, and how that can be used in the inter-conversion of cellulose polymorphs. Finally, chapter 5 discusses future outlooks and an overall conclusion.

Chapter 2

Cross-Coupling of Calix[4]pyrrole to an Organic Dye

Introduction

In 1886, Baeyer first synthesized octamethylcalix[4]pyrrole (**C4P**), a macrocycle composed of four pyrrole units, bridged together through condensation with four acetone units (Figure 10).[44] Calixpyrroles have a strong affinity for anions; for example, calix[4]pyrrole demonstrates a high affinity for fluoride (Table 1).[45,46] Functionalized calixpyrroles have been synthesized wherein selectivity and affinity can be fine-tuned for other chemical species. For example, octafluorocalixpyrrole (Figure 11A) has a significant increase in affinity towards anions compared to **C4P**, due to the increased dipole pulling electron density away from the N—H groups.[47] Pentapyrrolic calix[4]pyrrole has been shown to have an increased affinity for carboxylates such as acetate and benzoate, with K_a values on the order of magnitude of $>10^4\ M^{-1}$ (Figure 11B).[48] Bridged calixpyrroles have also been shown to have promise in developing sensors with heightened selectivity. A binol "strapped" **C4P** was developed that could bind carboxylates in an enantioselectivite fashion, with affinity towards (S)-2-phenylbutyrate being significantly higher than towards the R enantiomer (Figure 11C).[49] Other bridged calixpyrroles have been developed for a variety of host-guest chemistry applications.[50] Just

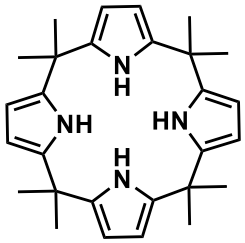

Figure 10. Calix[4]pyrrole (**C4P**)

Table 1. Association constants of **C4P** with various anions.

Anion	Binding Affninity to C4P (M^{-1})
F^-	17170
Cl^-	350
Br^-	10
$H_2PO_4^-$	97
Benzoate	196
Acetate	668

this year, a new functionalized calixpyrrole was developed that could sense for creatinine, a metabolite used to monitor kidney function, with a binding affinity (K_a) of 10^7 M^{-1} (Figure 11D).[51]

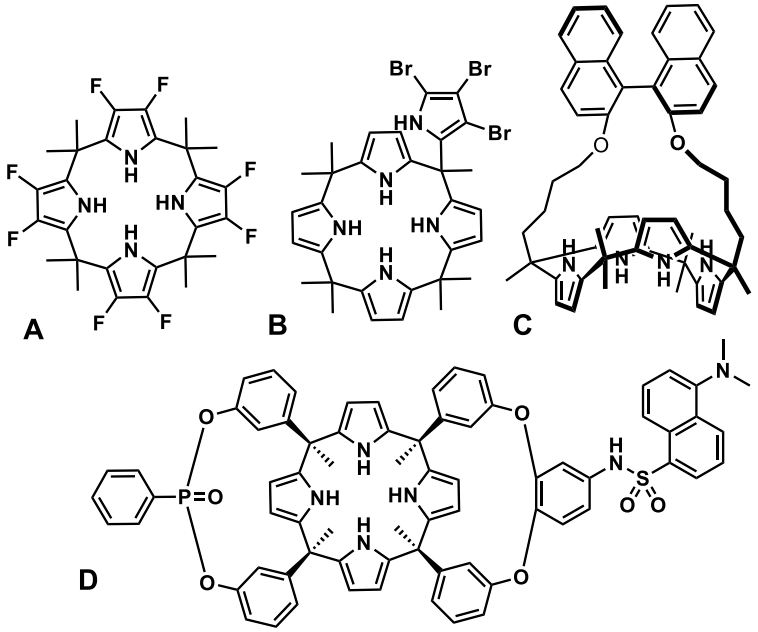

Figure 11. Various functionalized **C4P** molecules with enhanced recognition of distinct chemical species.

C4P has been functionalized extensively with organic dyes, enabling the development of colorimetric and fluorometric anion sensors. One of the first examples of this was in 2000 when Sessler and coworkers used a palladium-catalyzed Sonogashira coupling to conjugate **C4P** to a chromophore, enabling its use as a colorimetric sensor that could detect anions using UV/Vis spectroscopy. (Figure 12A)[52] Later that year, a class of "second generation" **C4P** anion sensors were developed from functionalization at its meso bridge. One such sensor was covalently bound to a fluorescein moiety, allowing for monitoring of anion recognition through fluorescence (Figure 12B). This sensor had a binding affinity of 10^6 M^{-1} for fluoride.[53] A few other examples of **C4P** being

functionalized at the meso bridge exist, with the attachment of other moieties such as coumarin[54] and BODIPY.[55] In 2006, Anzenbacher developed sensors through a Knoevenagel condensation between a formylated **C4P** and molecules with acidic protons α to electron withdrawing groups. One example made use of a diketone moiety for the condensation, which allowed for the formation of a sensor with a heightened affinity for

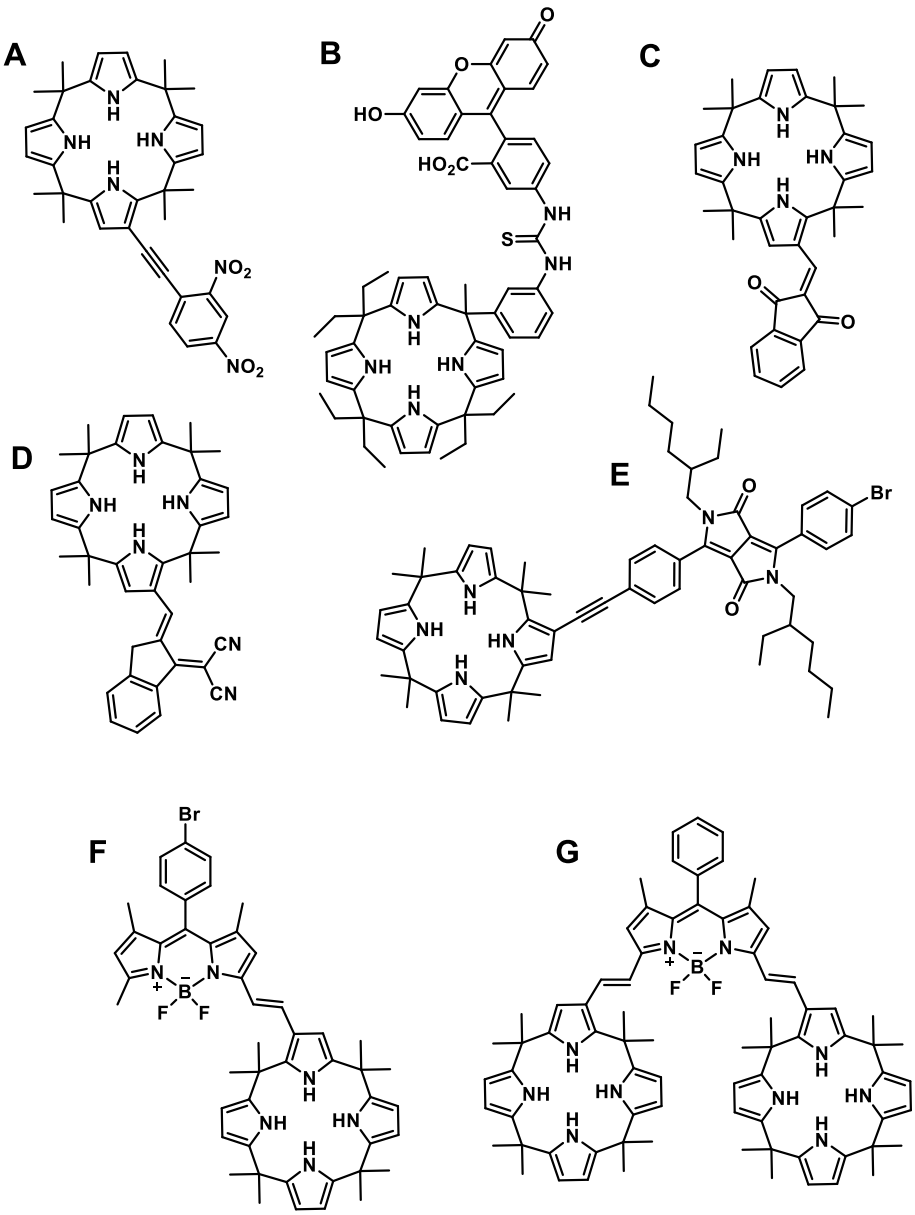

Figure 12. Anion sensors developed through the covalent attachment of chromophoric moieties to **C4P**.

anions relative to other **C4P** sensors, as the electron withdrawing diketone made one of the pyrrole H-atoms more electropositive (Figure 12C)[56]

Anzenbacher and coworkers synthesized cyano-containing **C4P** sensors for biologically-active carboxylates, such as ibuprofen and naproxen (Figure 12D).[57] More recently, fluorescent anion sensors have been developed through the Sonogashira coupling of diketopyrrolopyrrole to calixpyrrole (Figure 12E).[58] One of the most common organic dyes, BODIPY, has been conjugated to calix[4]pyrrole using a Knoevenagel condensation between a formylated calixpyrrole and the BODIPY methyl group.[59] The protons on the methyl group are acidic enough for a condensation because of the electron withdrawing BODIPY core. A mono-**C4P** BODIPY has been developed as an anion sensor, having similar binding affinities of **C4P** to species like fluoride, chloride, acetate, and dihydrogen phosphate (Figure 12F). An additional sensor making use of BODIPY has also been developed, as it takes advantage of both of the methyl groups on a BODIPY chromophore, attaching two calix[4]pyrrole units to it (Figure 12G). With two calix[4]pyrrole units in close proximity to one another, high affinity for aromatic dicarboxylates was observed.[60]

Motivation to Synthesize Polymeric C4P Anion Sensors

When in high concentrations, anions present in the environment are problematic pollutants. For example, excess chloride in the environment can corrode pipes and lead to crop damage. Overabundance of phosphates in pools of water can lead to algal blooms,

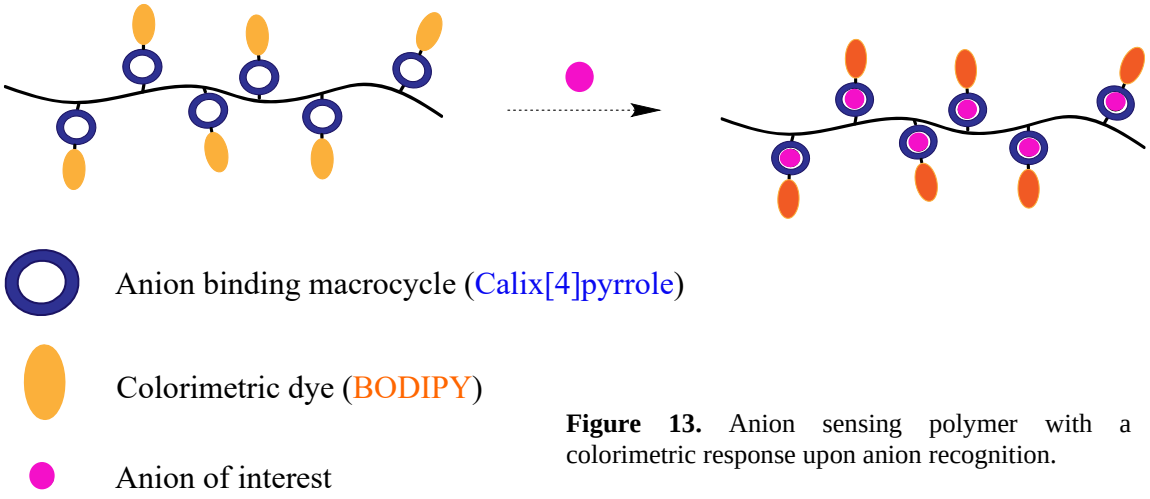

Figure 13. Anion sensing polymer with a colorimetric response upon anion recognition.

resulting in loss of aquatic life. Excess intake of fluoride in water can result in dental problems, and even lead to serious neurological problems.[61] Monitoring of these along with other toxic anions like cyanide are of extreme importance for society. Chemical tools need to be developed that monitor and remove anions (and other chemicals and toxins) from solution. This project aims to develop such tools by attaching calix[4]pyrrole in conjugation with a dye to a polymer as a pendant. **C4P** can bind anions, and the conjugation with a dye allows for ease of characterization, due to a colorimetric response (Figure 13). Polymers can be tuned to be removed from solution easily using precipitation. The first syntheses looked to take advantage of various methods to couple **C4P** to a diketopyrrolopyrrole (**DPP**) moiety, while also functionalizing either side with a handle for monomer / polymer attachment (Figure 14).

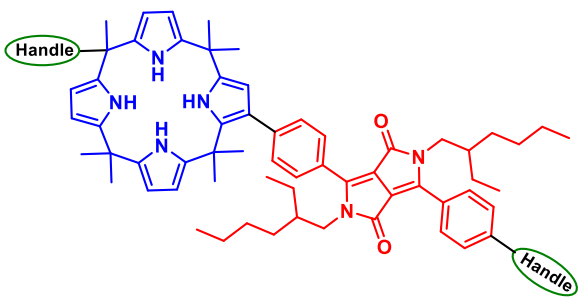

Figure 14. Potential **C4P-DPP** conjugate small molecule handles for polymer attachment.

Synthetic Pathways Toward C4P-Diketopyrrolopyrrole (DPP) Conjugates

The first synthetic route targeting a **C4P-DPP** conjugate with a handle took advantage of previous syntheses to make molecule **5** (Scheme 1), which demonstrated a colorimetric response upon anion recognition.[58] The Sonogashira coupling of **2** with trimethylsilyl acetylene proved difficult, as a competing dehalogenation mechanism took place in the presence of base.[62,63] Though yields were low, this route could still be pushed forward. It was hypothesized that the free aryl bromide present on **5** could be functionalized to a handle for polymer attachment. Two functionalization routes were, thus, envisioned to make use of azide-alkyne Huisgen cycloaddition. Substitution of the aryl bromide with an azide to generate **6** was attempted, however TLC showed that the product appeared to decompose too quickly to adequately isolate and characterize. The alternative was to

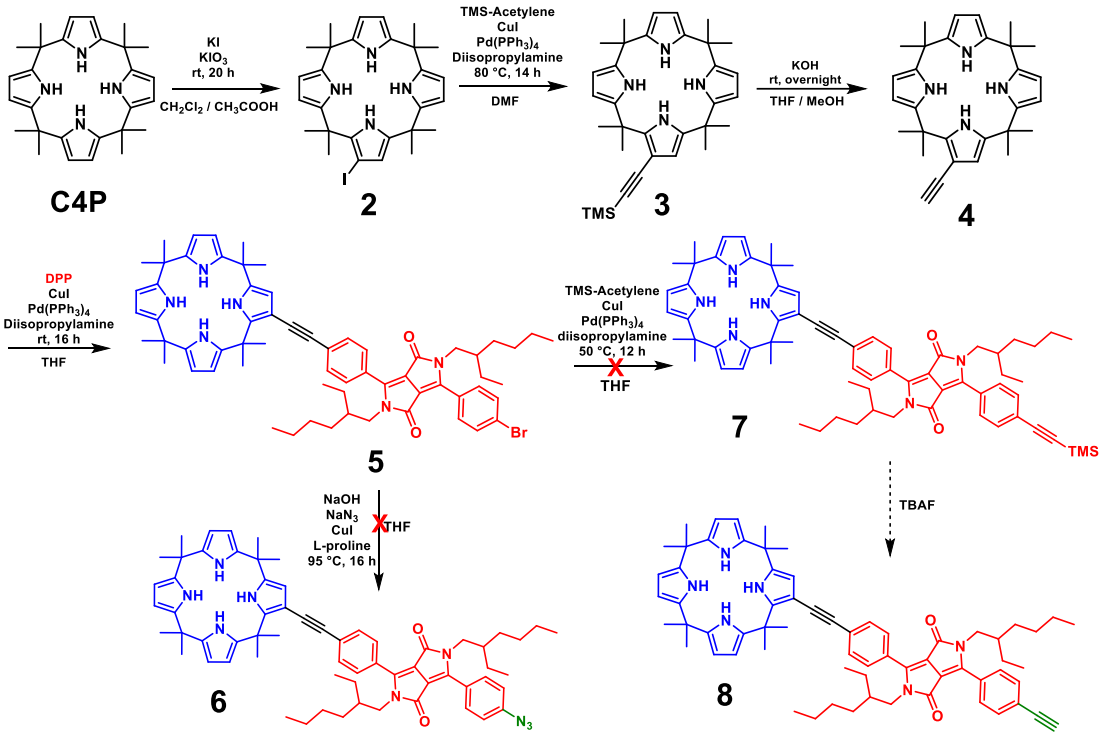

Scheme 1. Attempted functionalization of the aryl bromide in compound **5** to be used as a handle for polymer attachment.

generate an alkyne through Sonogashira coupling to afford **7**; however, the electron donating nature of the diketopyrrolopyrrole (**DPP**) dye combined with the potential binding of the calixpyrrole moiety to palladium slowed the oxidative addition when attempted.

Alternative endeavors aimed at functionalizing **DPP** before Sonogashira coupling with the **C4P** scaffold (Scheme 2). The first route made use of a Sonogashira coupling with 5-triethylsilylpentynol to make **9**. This coupling was achieved in a low 15% yield, likely due to the electronics of **DPP** slowing oxidative addition, as well as the formation of di-coupled product. The subsequent Sonogashira coupling of **9** with ethynyl **C4P 4**, was attempted but did not yield **10**. This is most likely owing to a combination of the **DPP** electronic nature along with coordination of the pyrrolic N—H moiety to the catalyst.

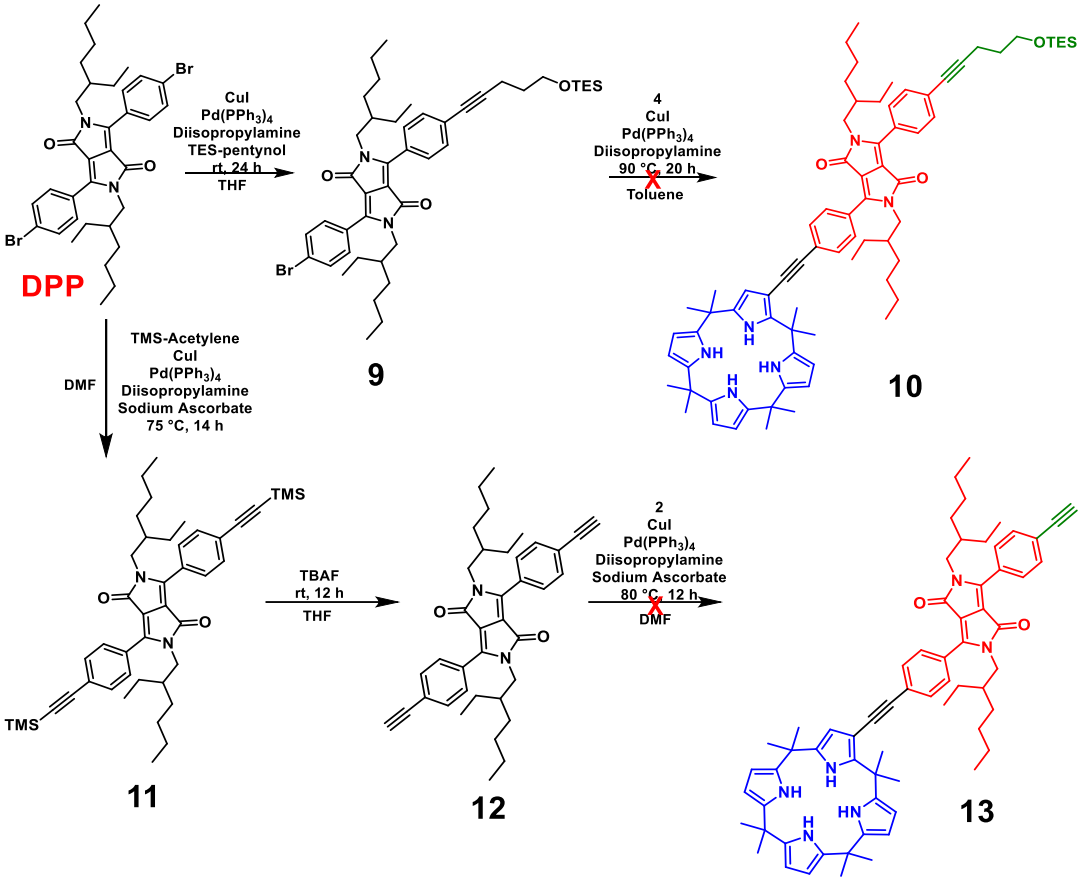

Scheme 2. Additional routes attempted using **DPP** as a handle.

Compound **10** would have been a great precursor to formation of a monomer, as the triethylsilyl ether could have been deprotected with fluoride and subsequently substituted into an acyl chloride monomer.

It was then thought that a Sonogashira coupling of **DPP** with trimethylsilyl acetylene to make **11**, which was achieved in 37% yield, could provide a more efficient alternative route, as functionalization of the **C4P** scaffold would be lessened. The subsequent deprotection of the trimethylsilyl alkynes could be achieved in moderate yield to form **12** after being subjected to TBAF. The subsequent mono Sonogashira coupling of **12** with iodinated calix[4]pyrrole **2** did not yield **13**, owing to the significantly competitive dehalogenation mechanism of pyrrole halides. Like previous targets, **13** would have been great for post polymerization azide-alkyne cycloaddition. The strategies employing Sonogashira couplings were not robust with these substrates, so a new route needed to be developed.

Toward Calix[4]pyrrole based Monomers

The next routes made use of previously-synthesized ethylhydroxy calix[4]pyrrole,[64] **14**, which could use the free alcohol present as a handle for polymer or monomer attachment (Scheme 3). Synthesis of **14** was low yielding, however grams of material could be made on a large scale, as reported. The free alcohol was subsequently protected with t-butyldimethylsilyl chloride to generate **15** in high yield, which would prevent various byproducts forming in subsequent steps. Compound **15** could be iodinated to form **16** in moderate yield, allowing for a future Suzuki-Miyaura coupling. Due to the

nonsymmetrical nature of the pyrrole carbon positions, **16** was isolated as a mixture of constitutional isomers, which was determined through ^{1}H, ^{13}C, and ^{127}I NMR spectroscopy. Nonsymmetrical **DPP 18** could be made in 3% yield over two steps, which proved to be an overall hindrance to this route due to the formation of two symmetrical byproducts, but it allowed for only one reactive site for subsequent cross-coupling reactions. A Miyaura

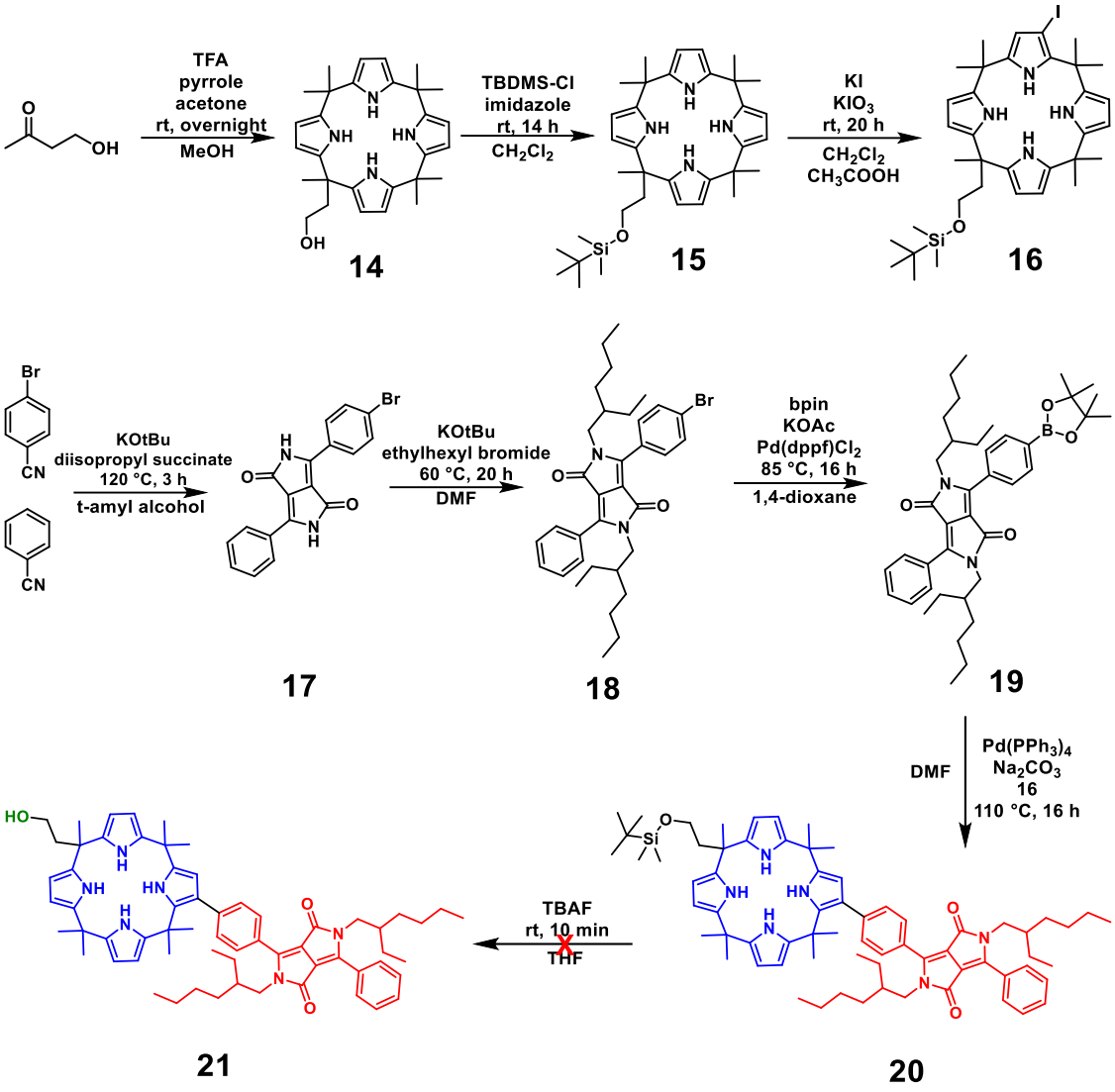

Scheme 3. Attempted synthesis of compound **21**, which made use of a handle on the calixpyrrole moiety. This would have been used to add to a monomer using acyl substitution.

borylation of **18** gave **19** in good yields. Optimal reaction conditions were determined after subjecting **DPP** to various borylation conditions and determining conversion through ^{1}H NMR spectroscopy (Scheme 4, Table 2). Compound **19** was then allowed to react with **16** through Suzuki-Miyaura coupling, which generated **20** in a 7% yield at best. This low reactivity was due to the competing dehalogenation mechanism of the iodinated pyrrole, along with the reduced reactivity of the bis(pinacolato)diboron ester as opposed to boronic acids and other boronic esters.[65] Compounds **18**, **19**, and **20** were characterized with UV/vis and fluorescence spectroscopy to determine their similarity to previously reported **DPP** systems. The absorption spectra collected for all three compounds resulted in an excitation maxima at 475 nm in THF (Figure 15). They also exhibited emission maxima of 540 nm (Figure 16). Both of these results are consistent with similar previously reported **DPP**s.[15] Silyl deprotections with fluoride are typically efficient reactions, but the deprotection of **20** was unsuccessful, as significant decomposition of the **DPP** dye was observed. Upon addition of TBAF, the reaction mixture lost both its color and fluorescence. The

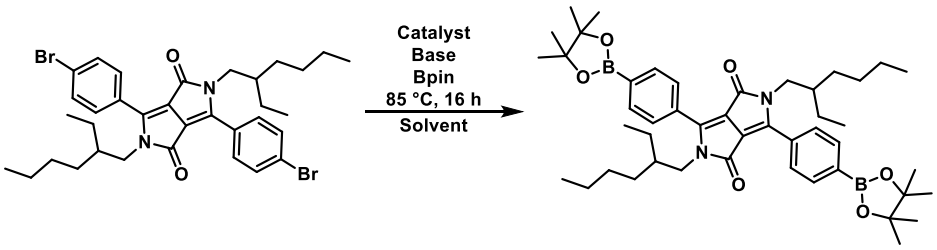

Scheme 4. General conditions for borylation of **DPP**.

Table 2. Screened Conditions used in the borylation of **DPP**

Base	Catalyst	Solvent	Conversion
KOAc	$Pd(PPh_3)_4$	1,4-dioxane	99 %
KOAc	$Pd(dppf)Cl_2$	1,4-dioxane	98 %
KOtBu	$Pd(dppf)Cl_2$	Toluene	76 %
KOAc	$Pd(OAc)_2$	DMF	74 %

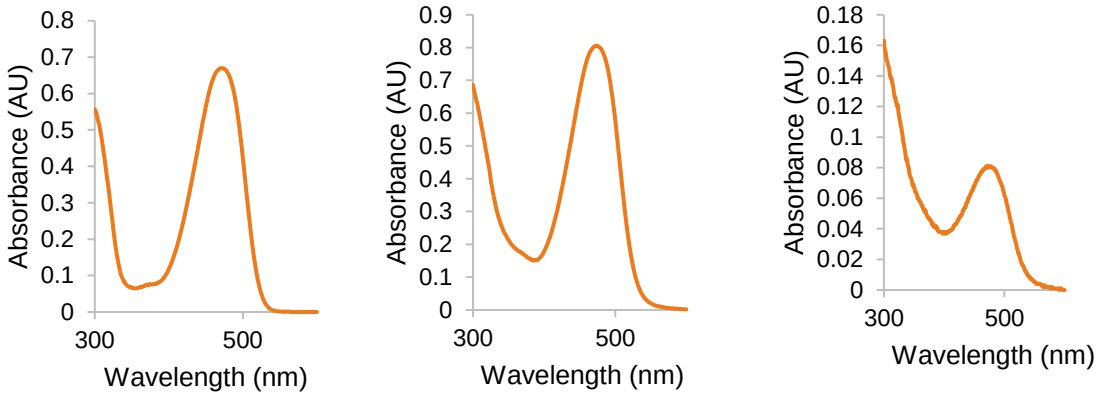

Figure 15. UV/Vis spectra of compounds **18** (left), **19** (middle), and **20** (right) in THF (50 µM).

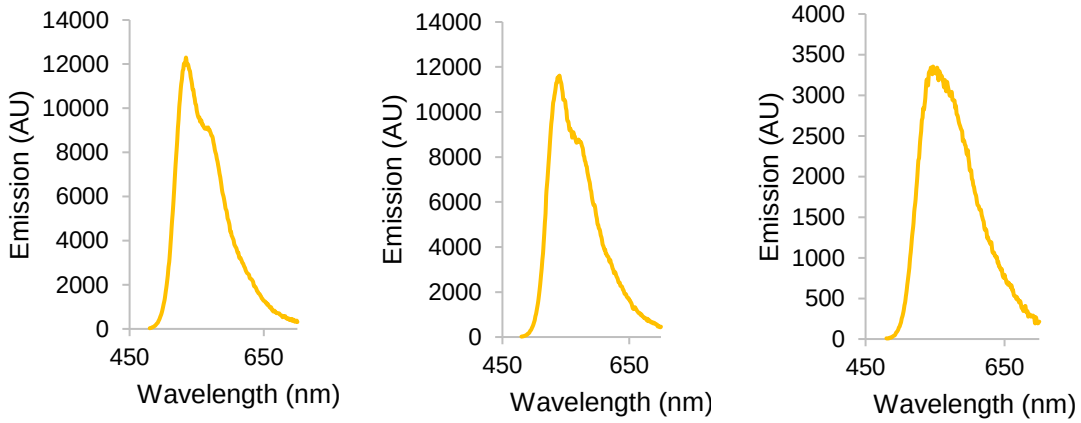

Figure 16. Emission spectra of compounds **18** (left), **19** (middle), and **20** (right) (50 µM). Ex. 475

decomposition was probed by NMR spectroscopy, and was observed in as few as five minutes. The stability of symmetrical **DPP** was then assessed in the presence of TBAF, hydrazine, and $NaBH_4$, as each of these could be used for deprotection for either a nucleophilic alcohol or amine. **DPP** was determined to decompose regardless of which reagent was used, as determined by ^1H NMR spectroscopy and qualitative assessments of the color and fluorescence changes. Hydrazine or $NaBH_4$ would have been used to deprotect a phthalimide to an amine, which if completed would have been a better nucleophile for post-polymerization modification reactions. A route designed to allow for

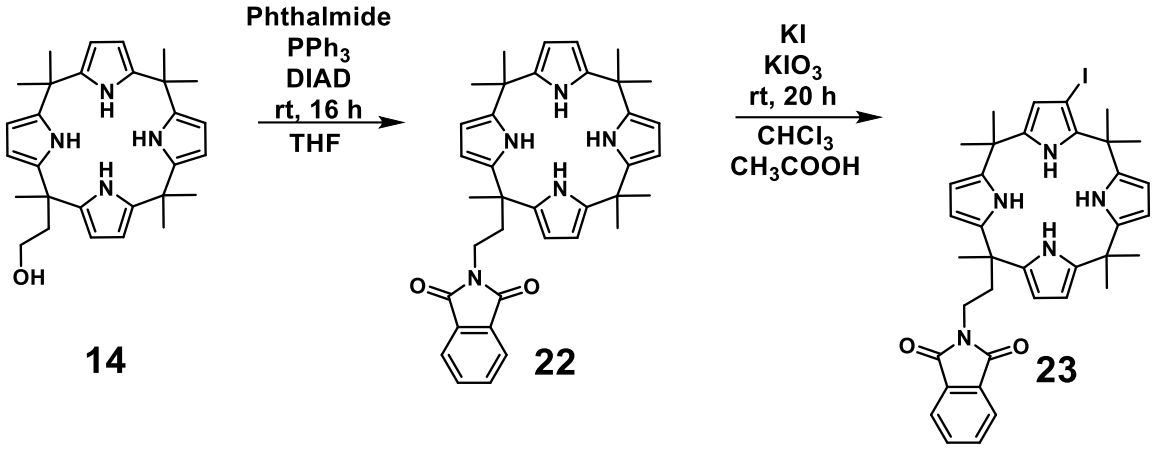

Scheme 5. Mitsunobu reaction of **14** to form **22** and subsequent iodination.

the use of a free amine was started, in which the compounds **22** and **23** were both made successfully through a Mitsunobu reaction with **14** followed by an iodination (Scheme 5).

Investigating a BODIPY Organic Dye for Cross-Coupling Reactions

The problems associated with the **DPP** dye (low yields and decomposition) rendered the decision to try a new dye, such as BODIPY. It was envisioned that a BODIPY dye with an aryl bromide could be functionalized through a Suzuki-Miyaura coupling, or coupled with an alkyne via Sonogashira coupling. Synthesis of this functionalized BODIPY was a straightforward approach that started with the synthesis of dipyrromethane **24** in 94% yield from a condensation between pyrrole and 4-bromobenzaldehyde (Scheme 6). Subsequent oxidation followed by addition of the BODIPY core to make **25** was achieved in a modest yield. The following Miyaura borylation could be achieved using previous conditions to make **26** in moderate yield. Compound **26** could then react with **2** through a Suzuki-Miyaura coupling. It was decided to use compound **2** because the small molecule without the handle would be easier to characterize, and because we had more of

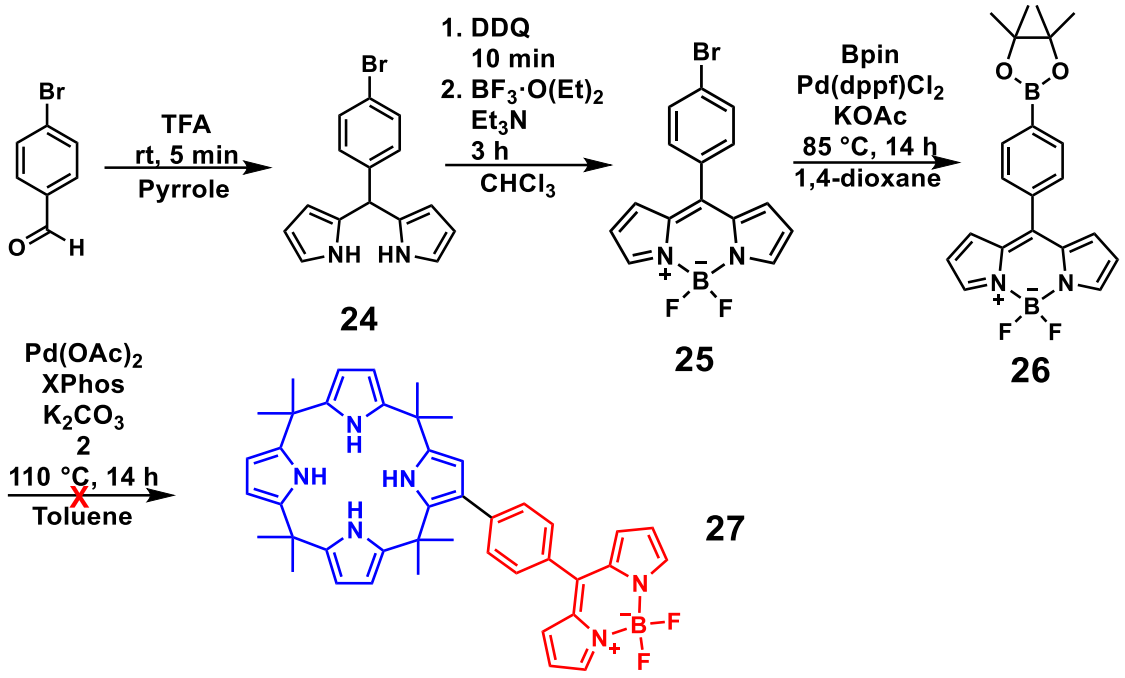

Scheme 6. Attempted synthesis of small molecule compound **27**.

compound **2** to use. This attempted Suzuki-Miyaura coupling did not yield **27**, due to the dehalogenation mechanism previously mentioned, along with potential calixpyrrole coordination with the catalyst. It was postulated that the BODIPY core could also cause issues with Suzuki couplings, so coupling conditions were screened with BODIPY **26** in the presence of 4-bromobenzaldehyde to determine the utility of BODIPY for this reaction (Scheme 7). Percent conversions were between 71 and 81% as determined by ^{1}H NMR

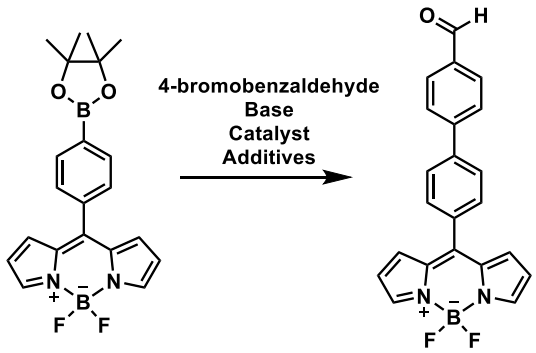

Scheme 7. General conditions to determine optimal Suzuki-Miyaura coupling conditions.

spectroscopy (Table 3). Additionally, TLC confirmed the formation of a new fluorescent aldehyde. All of these conditions were used in additional attempts to make compound **27**, but with no apparent conversion. It appeared that the BODIPY scaffold was not affecting the cross-coupling reactions, leaving the calixpyrrole moiety as the only culprit for such low yields, if any. The change to BODIPY helped to simplify the route, but problems with cross-coupling still remained, suggesting that routes limiting these reactions should be considered.

Table 3. Optimization table of Suzuki-Miyaura conditions of borylated BODIPY **26** and 4-bromobenzaldehyde.

Base	18-crown-6	Catalyst	Conversion
KHMDS (2 equiv.)	2 equiv.	$Pd(OAc)_2$ (1 mol%) / Xphos (2 mol%)	76 %
KHMDS (2 equiv.)	0 equiv.	$Pd(PPh_3)_4$ (5 mol%)	81 %
KHMDS (2 equiv.)	2 equiv.	$Pd(PPh_3)_4$ (5 mol%)	72 %
K_2CO_3 (2 equiv.)	2 equiv.	$Pd(OAc)_2$ (1 mol%) / Xphos (2 mol%)	72 %
K_2CO_3 (2 equiv.)	0 equiv.	$Pd(PPh_3)_4$ (5 mol%)	71 %

Conclusion

All of the aforementioned routes proved to be inefficient due to extremely low yields, especially in cross-coupling reactions. The low yields were caused primarily by dehalogenation of calix[4]pyrrole halides, as well as possible coordination of the N-atoms of pyrrole to the Pd catalyst. It was determined that even though cross-coupling reactions can work on **C4P** substrates, these reactions were difficult to optimize for my multi-step syntheses, mostly due to a competing dehalogenation mechanism. Due to the problems associated with calixpyrrole in cross coupling reactions, a completely new route needed to be developed to achieve the aim of this project, which was to develop polymeric anion sensors through the attachment of a **C4P**-dye conjugate to a polymer.

Chapter 3

Synthesis of Polymer-Calix[4]pyrrole-BODIPY Conjugates

Introduction

Calixpyrrole (**C4P**) has been effectively appended to polymer side chains; yet less has been done on this than the development of colorimetric anion sensors. In 2008, Sessler and coworkers made the first random copolymer of methyl methacrylate (MMA) and a **C4P**-based monomer (Figure 17A).[66] This copolymer was used to extract both fluoride and chloride, in the form of their tetrabutylammonium salts. Though they did not discuss binding affinity, they noted that ^{1}H NMR spectroscopy showed that extractions of chloride gave a greater downfield shift in pyrrole N—H signals than did fluoride, which they attributed to the Hofmeister bias. Later that year, the Sessler group developed a new PMMA random copolymer that had both **C4P** and benzo-15-crown-5-ether pendants (Figure 17B), which was used to more efficiently extract potassium halides from solution than their previous polymer.[67] **C4P** has also been appended to a poly(styrene) backbone through post-polymerization

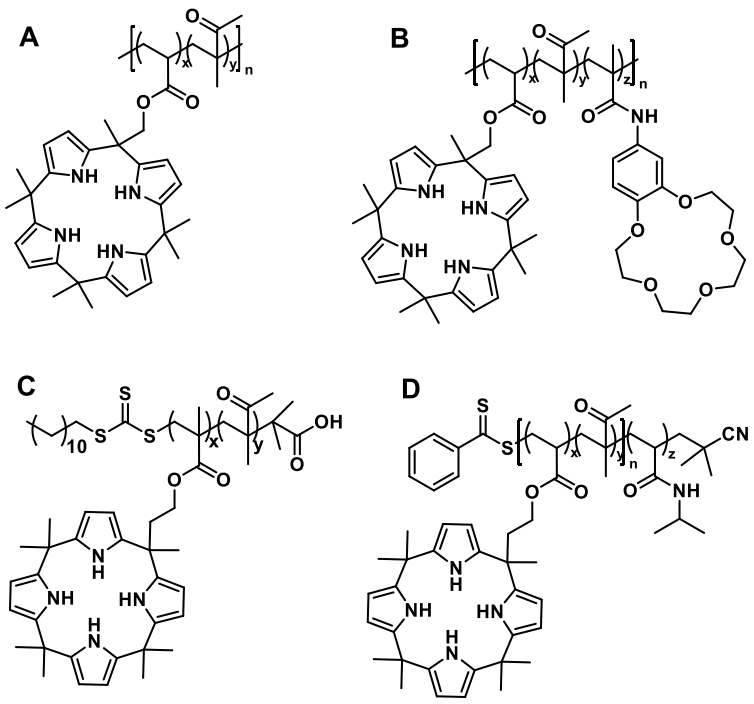

Figure 17. Previously reported polymers with calix[4]pyrrole pendants.

azide-alkyne click reaction.[68] More recently, Sessler used an MMA copolymer containing **C4P** side-chains that could be crosslinked using aromatic diacetate anions, which they used to modulate viscoelastic properties (Figure 17C).[64] This was the first example of reversible addition-fragmentation chain-transfer (RAFT) polymerization being used to develop polymers bearing **C4P** side-chains. Further, methacrylate **C4P** copolymers containing Pt(II)-bound porphyrin pendants were used to intramolecularly crosslink in the presence of terephthalate to form phosphorescent single chain polymer nanoparticles.[69] More recently, copolymers were made using methyl methacrylate, N-isopropylacrylamide (NIPAM), and **C4P** pendants (Figure 17D). These amphiphilic copolymers were used to capture and remove anions from solution, as they would precipitate out from water when heated.[70] The researchers were also able to recycle their polymer, which highlighted the potential of polymers bearing **C4P** side-chains to be used for environmental remediation. This chapter will focus on how a new scheme was developed that was successful at incorporating a **C4P**-dye conjugate into side chains of a polymer. Herein, a functional polymeric fluoride sensor with BODIPY-**C4P** conjugate pendants is disclosed. Up to this point, colorimetric **C4P** anion sensors have not been incorporated into polymeric systems. The incorporation of a BODIPY-**C4P** conjugate side-chain onto this polymer enables ease of fluoride detection with UV/vis and fluorescence spectroscopy.

Utilization of a Knoevenagel Condensation for Monomer Design

A different route was developed that featured the Knoevenagel condensation of **C4P** with a methylated BODIPY (Scheme 8). This started with a previously reported[71] one-pot synthesis of **29** in moderate yield. Phenol **29** was then converted to a TBDMS ether

in 99% yield. Next, aldehyde **31** was formed from **C4P** using a Vilsmeier-Haack formylation, and resulted in 11% yield. Aldehyde **31** degrades quickly, so the Knoevenagel condensation between **31** and BODIPY **30** needed to be set up promptly after successful purification of **31**. The condensation successfully yielded the BODIPY-**C4P** conjugate **32** in 8% yield. The low yield could have been because of decomposition of compound **31** prior to use, as well as observed cleavage of the silyl ether. The subsequent deprotection was efficient, as aryl TBDMS ethers can be cleaved with potassium hydroxide very quickly at room temperature,[72] resulting in a 93% yield, uncovering phenol **33**. The phenol was

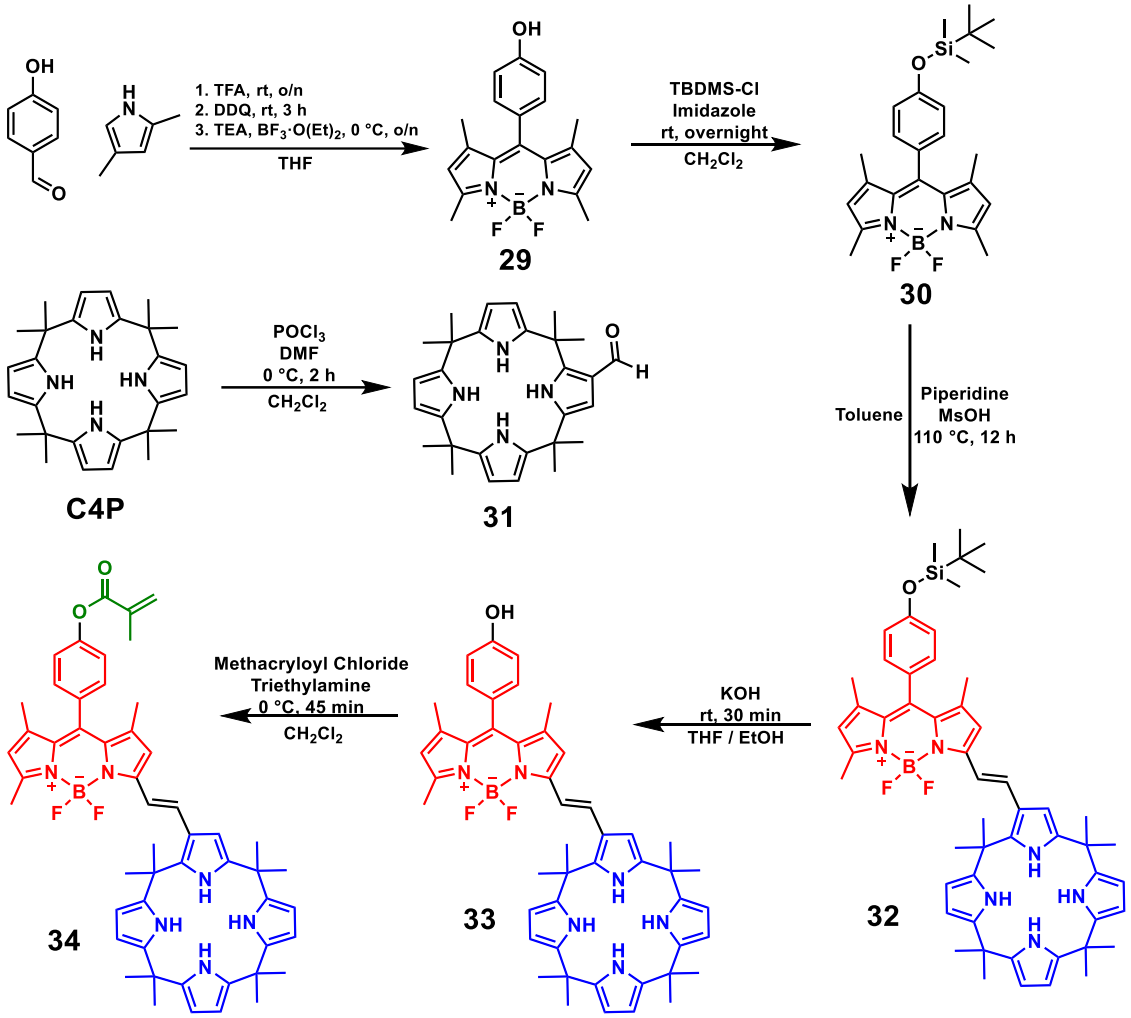

Scheme 8. Synthesis of Monomer **34**

then allowed to react with methacryloyl chloride in an acyl substitution to yield monomer **34** in 60% yield. With the targeted monomer in hand, the next step was to synthesize a random copolymer of **34** with methyl methacrylate.

RAFT Polymerization of Monomer 34 with Methyl Methacrylate

Random copolymers containing BODIPY-**C4P** were synthesized using RAFT polymerization. MMA was utilized as the comonomer with AIBN as a radical source and 4-cyano-4-[(dodecylsulfanylthiocarbonyl)sulfanyl]pentanoic acid as the RAFT chain transfer agent (Scheme 9). The reaction was allowed to stir at 80 °C for 14 hours and then stored in the freezer for 10 minutes to quench the polymerization. After quenching the reaction, the polymer was purified through reprecipitation in diethyl ether. GPC analysis on the polymer resulted in a Mn of 16,670 Da and a dispersity of 1.15

The loading ratio of MMA to BODIPY-**C4P** was 19:1, thus targeting 5% incorporation of the sensor pendant. ^{1}H NMR spectroscopy was used to determine the ratio of MMA to sensor pendants (Figure 18). A ratio of 33:1 was calculated through comparison

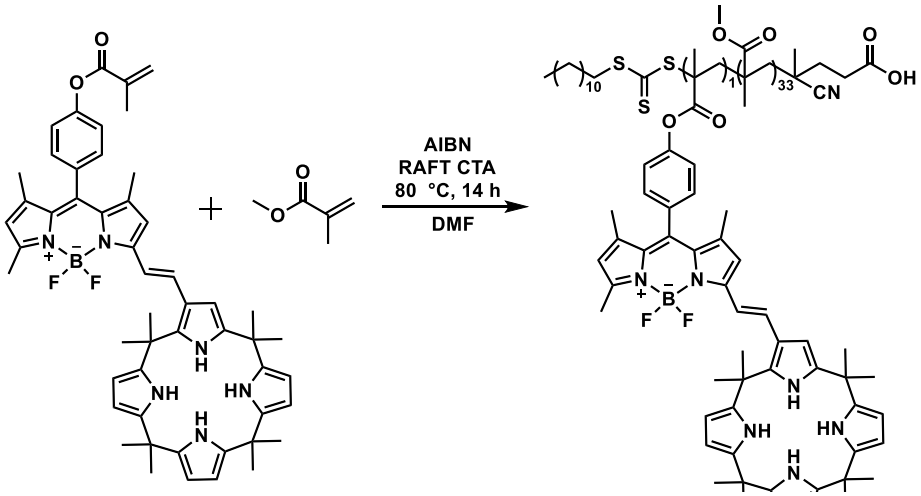

Scheme 9. RAFT Polymerization of **34** with MMA to yield **Poly(BODIPY-C4P)**

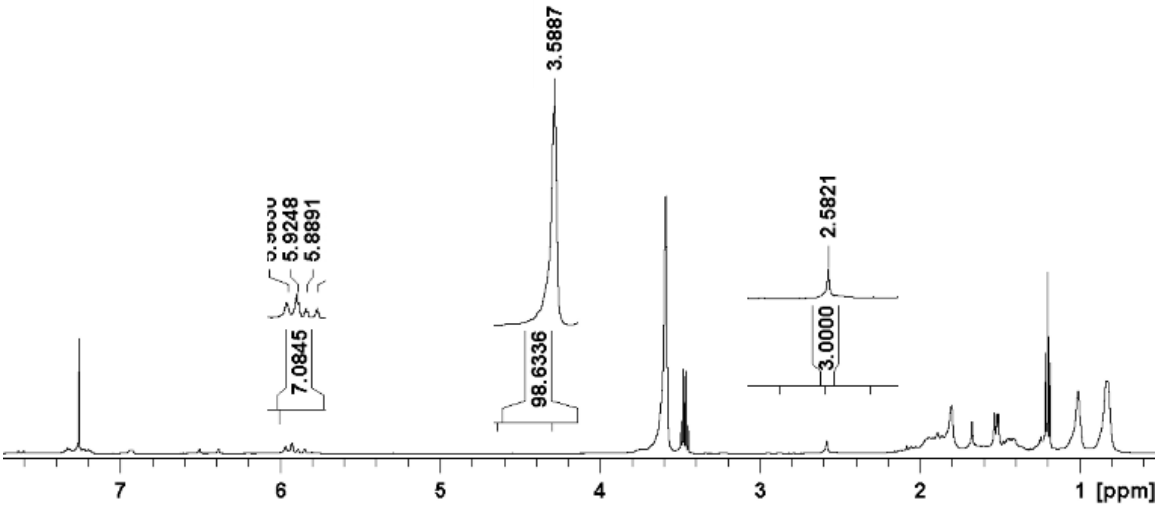

Figure 18. ^{1}H NMR of **Poly(BODIPY-C4P)**

of the BODIPY methyl group (2.58 ppm) to the methyl ester of MMA (3.59 ppm). Additionally, a multiplet ranging from 5.85 – 5.97 ppm integrated to seven protons, indicating retention of the integrity of the BODIPY-**C4P** conjugate (Figure 18). The resultant ratio deviation (compared to the target) was attributed to the likely difference in radical reactivity of the BODIPY-**C4P** monomer compared to MMA. This ratio would be used later to determine the concentration of sensor pendants relative to polymer.

UV/Vis and Fluorescence Spectroscopy of Poly(BODIPY-C4P)

The optimal solvent for UV/vis and fluorescence titration was then determined. We chose solvents with a broad range of dielectric constants, as it might be expected that ion binding capacity and affinity would be impacted by solvent choice. Thus, we used $CHCl_3$, THF, MeCN, and DMF. There was an apparent bathochromic shift in absorbance as the polarity of solvents was increased from $CHCl_3$ (Figure 19A). The color of **Poly(BODIPY-C4P)** was magenta when dissolved in $CHCl_3$, and shifted to a deep blue in the more polar

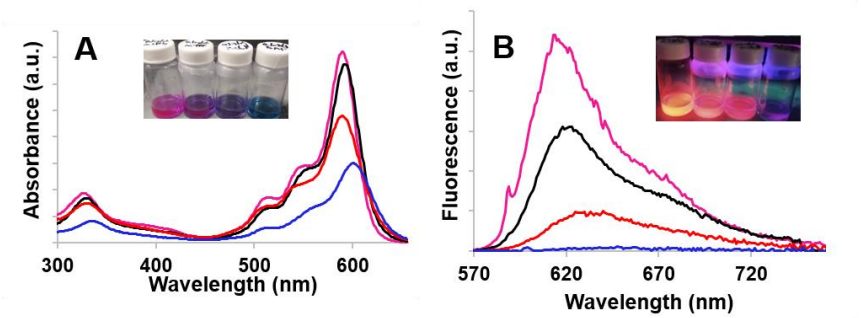

Figure 19. **A** UV/Vis spectra of **Poly(BODIPY-C4P)** (0.1 mg/mL, 2.29 x 10^{-5} M **BODIPY-C4P** pendants) in $CHCl_3$ (magenta), THF (black), MeCN (red) and DMF (blue). Vials shown from left to right show $CHCl_3$, THF, MeCN, and DMF. **B** Emission spectrum of **Poly(BODIPY-C4P)** in $CHCl_3$ (magenta, 0.01 mg/mL), THF (black, 0.01 mg, mL), MeCN (red, 0.1 mg/mL), and DMF (blue, 0.1 mg/mL). Vials from left to right show $CHCl_3$, THF, MeCN, and DMF.

(higher dielectric) solvent DMF (Figure 19A). As solvent polarity increased, the fluorescence was visibly quenched (Figure 19B). Indeed, fluorescence was quenched so dramatically in MeCN and DMF that concentrations of 0.01 mg/mL of the polymer gave little to no signal when compared to in $CHCl_3$ and THF. Even when MeCN and DMF were at concentrations of 0.1 mg/mL they gave signals significantly lower than that of their less polar, more dilute counterparts. Figure 19B shows this pronounced quench in fluorescence. The shifts in the UV/vis spectra and quenching of fluorescence could be due to solvent effects on the BODIPY core, as previous BODIPY scaffolds have shown significant quenching of their emission as solvent polarity is increased.[73,74] It is suspected that these observations could also be due to solvent recognition onto the **C4P** scaffold because there are previous reports that calix[4]pyrrole can bind to neutral polar species, such as DMF.[28]

UV/Vis and Fluorescence Titrations of POLY(C4P-BODIPY) with Fluoride

The utility of **poly(BODIPY-C4P)** as a colorimetric fluoride sensor was assessed, and compared to small molecule counterparts for binding affinity. Upon titration with tetrabutylammonium fluoride (TBAF), the observed shifts in absorbance were similar to

that of previous small molecule BODIPY-**C4P** anion sensors (Figure 20A).[55] In particular, the peak at 590 nm diminished while a new peak at 605 nm grew. The association constant of the pendant sensors was determined to be 1.8 x 10^4 M^{-1} using absorbance shifts. We also observed significant quenching of fluorescence upon titration with TBAF (Figure 20B). The shifts in absorbance and quenching of fluorescence are attributed to intramolecular charge transfer upon fluoride recognition. The association constant determined from fluorescence quenching was 4.5 x 10^4 M^{-1}. Association constants were determined using Bindfit.[75,76] Previously reported small-molecule BODIPY-**C4P** conjugates demonstrated a binding affinity towards fluoride of ca. 7 x 10^4 M^{-1}.[55] The binding affinities of the BODIPY-**C4P** polymer are consistent in magnitude with previous calix[4]pyrrole literature, wherein small differences overall are likely owing to the influence of the very nonpolar main-chain of the polymer, as it would be less likely to interact with species of high charge density. Despite subtle differences, the high fluoride affinity demonstrates that **poly(BODIPY-C4P)** can be used as an efficient sensor. Thus, it has the potential for future use in the design of sensors tuned for solubility in targeted systems, such as polluted

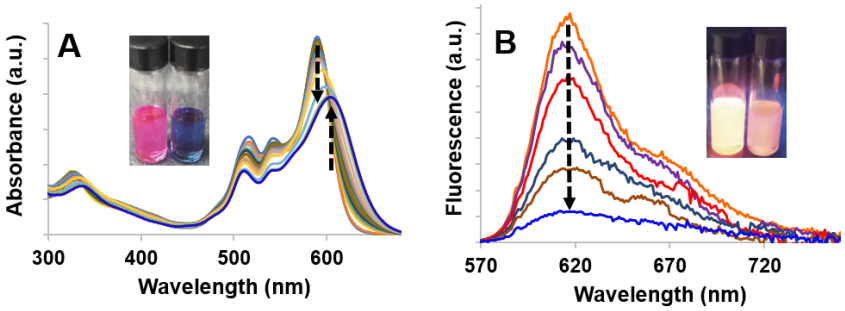

Figure 20. **A** UV/vis spectroscopic titrations of **Poly(BODIPY-C4P)** at 0.1 mg/mL (2.29 x 10^{-5} M calixpyrrole pendants) with TBAF (0 M to 3.44 x 10^{-4} M). Vials show the color change from magenta (0 equiv. TBAF) to blue (10 equiv. TBAF). **B** fluorescence titrations of **P1** (0.01 mg/mL) with TBAF (0 M to 6.88 x 10^{-5} M). Vials show quench in fluorescence from left (0 equiv. TBAF) to right (10 equiv. TBAF).

aqueous systems. Additionally, tuning towards more selective anions could be achieved through additional functionalization of the calix[4]pyrrole scaffold, or through the addition of crosslinks, which would enable selectivity due to the hydrophobic effect.

Conclusion

The route that conjugated calix[4]pyrrole to a BODIPY dye through a Knoevenagel condensation proved to be more efficient than previously attempted cross-coupling routes. The use of a phenolic handle on the BODIPY scaffold allowed for facile attachment to a monomer. Copolymers were synthesized with BODIPY-**C4P** side-chains, which allowed for fluoride detection in $CHCl_3$. The binding affinity of **poly(C4P-BODIPY)** was on the same order of magnitude for fluoride recognition as previously reported **C4P** sensors. Modification of future polymeric scaffolds with this BODIPY-**C4P** pendant will allow for the design of sensors that could have heightened selectivity for specific anions, have unique material properties, and most importantly remove anions from aqueous systems without use of organic solvents.

Chapter 4

Modifying Hydrogen Bonding Interactions in Cellulose Polymorphs

Introduction

While the development of synthetic polymer systems capable of noncovalent interactions is important, studying supramolecular interactions of natural polymers is important as well. Cellulose is a widely used natural polymer that is made up of repeating glucose units connected by β-1,4-glycosidic bonds (Figure 21).[77,78] Each glucose unit has three hydroxy groups present, which facilitates the formation of intermolecular O—H··O hydrogen bonds between cellulose chains. In addition to these hydrogen bonds, cellulose has a longitudinal dipole going from its non-reducing end towards its reducing end, as well as a transverse dipole perpendicular to the chain. The presence of hydrogen bonding interactions along with the aforementioned dipoles gives rise to piezoelectric properties.[79]

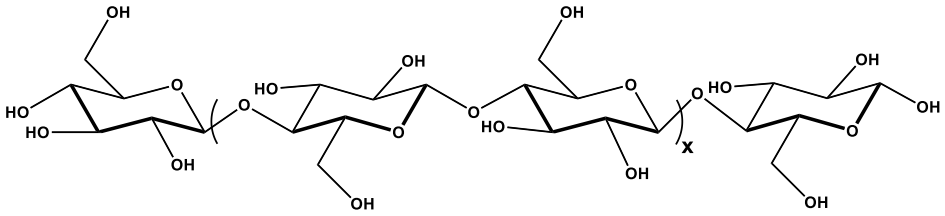

Figure 21. Chemical Structure of Cellulose

Piezoelectricity in cellulose is not well understood, unlike in synthetic materials such as poly(vinylidene fluoride) and perovskite lead zirconate titanate. Previous reports of transverse piezoelectric coefficients in cellulose have ranges that differ by six orders of magnitude and longitudinal piezoelectric coefficients that differ by two orders of magnitude.[80] It is believed that this substantial range is due to the differences in alignment (and thus, polarity) of cellulose nanocrystals of different polymorphs or sources. Finding a way to align the nanocrystals within cellulose, would allow for the development of

materials with ideal piezoelectric properties from naturally abundant and biodegradable sources.

To achieve this, we planned to investigate hydrogen bonding interactions between cellulose and primary amines. Cellulose can exist as a handful of different polymorphs, with cellulose-Iβ being the most common in plants.[81] Conversion of cellulose-Iβ to cellulose-III has been reported to occur in the presence of liquid ammonia (Figure 22).[82] In

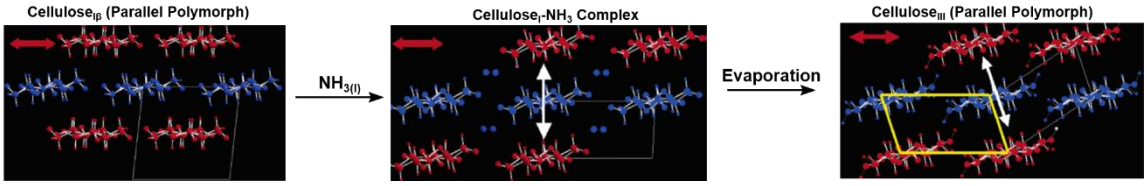

Figure 22. Process of converting cellulose-Iβ to cellulose-III using ammonia.[82]

this process, liquid ammonia is introduced, disrupting the intrinsic hydrogen bonding between cellulose chains and making a cellulose – ammonia complex. Upon evaporation of ammonia, cellulose-III, a polymorph where the chains are not stacked linearly, is retained. An additional reported method to make cellulose-III is to 'swell' cellulose-Iβ with ethylenediamine to make a cellulose – ethylenediamine complex, and subsequently wash the amine away with methanol.[83] Swelling refers to making the individual polymers within the cellulose lattice move further away from each other (as opposed to the compactness of the original hydrogen bonding), thus making the overall structure volume appear 'swollen.' Interestingly enough, washing the cellulose – ethylenediamine complex with water converts the cellulose back to cellulose-Iβ, likely because while swollen there is enough room for water to disrupt the lattice and hydrogen bond with chains, causing them to slip into the original network easily.[82]

Additionally, the cellulose – ethylenediamine complex can be isolated by evaporation of excess ethylenediamine with a nitrogen stream. Other reports show that cellulose-III can be converted to cellulose-Iβ through combinations of water and heat, usually using boiling water to achieve this transformation (Figure 23).[84,85] Each of these

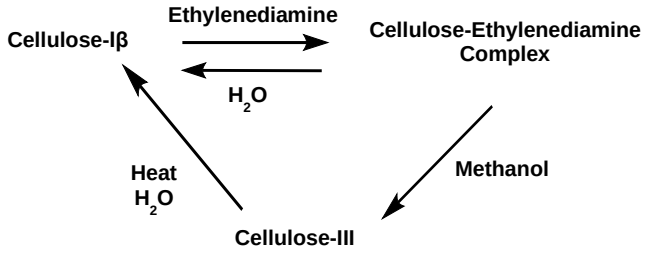

Figure 23. Methods to convert cellulose to different conformations of cellulose-Iβ, cellulose – ethylenediamine complex, and cellulose-III.

transformations have been characterized by X-ray diffraction (XRD).[86] Cellulose nanocrystals have also undergone these polymorph transformations,[87] and have been shown to align in the presence of external magnetic fields of 1.2 T as well as external electric fields 2000 V/cm.[88,89] We hypothesized that while 'swollen' by different primary amines, we could align the cellulose nanocrystals within cotton.

Testing Amines for Swelling Capabilities

The first steps involved were to determine which amines could swell the cellulose. We tested ethylenediamine, 1,2-diaminopropane, 1,3-diaminopropane, propylamine, and ethanolamine. It was found that smaller diamines such as ethylenediamine, 1,2-diaminopropane, and 1,3-diaminopropane were able to convert cellulose-Iβ to cellulose-III after swelling and methanol washing (Table 4). A cellulose – amine complex was observed

Table 4. Scope of amines used to convert cellulose-Iβ cotton balls to cellulose-III.

Amine	H_2O Wash	N_2 Wash	MeOH Wash
Ethylenediamine	Cellulose-Iβ	Cellulose – Amine Complex	Cellulose-III
1,2-diaminopropane	Cellulose-Iβ	Cellulose – Amine Complex	Cellulose-III
1,3-diaminopropane	Cellulose-Iβ	Cellulose – Amine Complex	Cellulose-III
Propylamine	Cellulose-Iβ	Cellulose – Amine Complex	Cellulose-Iβ
Ethanolamine	Cellulose-Iβ	Cellulose-Iβ	Cellulose-Iβ

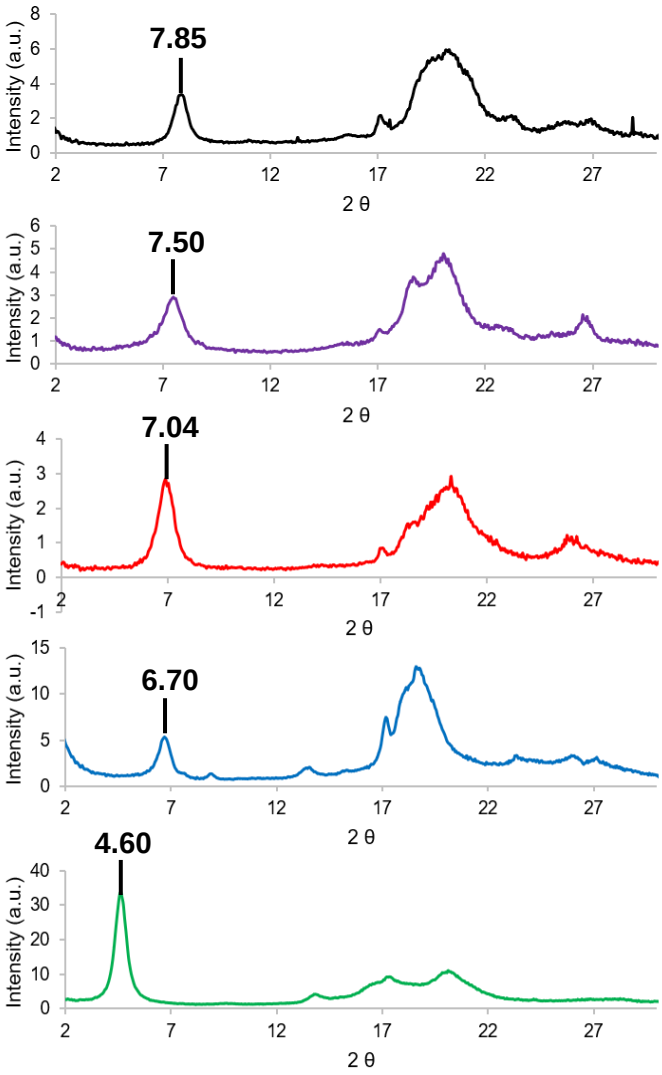

Figure 24. X-ray diffraction profiles of cellulose – amine complexes. Ethylenediamine (black), 1,2-diaminopropane (purple), 1,3-diaminopropane (red), 1,2-diaminocyclohexane (blue) and trans-1,4-diaminocyclohexane (green).

after evaporation of all of the aforementioned solvents as well as with propylamine, as confirmed by XRD (Figure 24). Strangely, swelling with ethanolamine did not result in any observed cellulose-III or cellulose – amine complex, suggesting two -NH_2 groups (as opposed to a mix of NH_2 and OH) are required. Thus, only the diamines could efficiently convert to cellulose-III. Next, we investigated larger diamines, as this increased distance could allow for more

degrees of freedom for rotation while in the swollen state.

In total, we isolated cellulose – amine complexes of five different diamines. As the size of the diamines was increased, we noticed a decrease in 2θ (Figure 24). This decrease in the incidence angle corresponds to an increase in d-spacing. This makes sense, as larger distances between cellulose chains should result when the length of the chain between amine functionalities increases. The peak indicative of the cellulose – amine complex is at 7.85 for ethylenediamine, and shifts dramatically to 4.60 in trans-1,4-diaminocyclohexane. It was hoped that this large shift would enable the use of trans-1,4-diaminocyclohexane in the magnetic and electric field alignment experiments, but this diamine along with 1,2-diaminocyclohexane were not able to be fully converted to cellulose-III. Because of this, these diamines were not used for alignment experiments. We also decided that 1,3-diaminopropane was likely too corrosive to be used in alignment experiments.

Attempt to Align Cellulose Using External Fields

We found that cotton twine has some degree of alignment to it (Figure 25), and decided to use it in the experiments, as monitoring the rotation of the cellulose nanocrystals within the twine would be straightforward. The first attempt at alignment was using an external electric field. We first tried applying 100 V while the twine was in between two stainless steel plates 1 mm apart, all while submerged in either ethylenediamine or 1,2-diaminopropane, giving a field of 100 V/mm. We noticed that upon application of the field, the voltage immediately dropped to

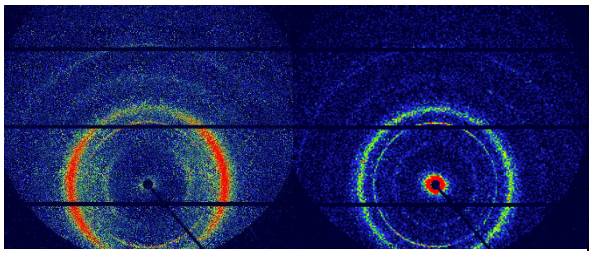

Figure 25. X-ray diffraction pattern of cotton twine (left) and cotton ball (right).

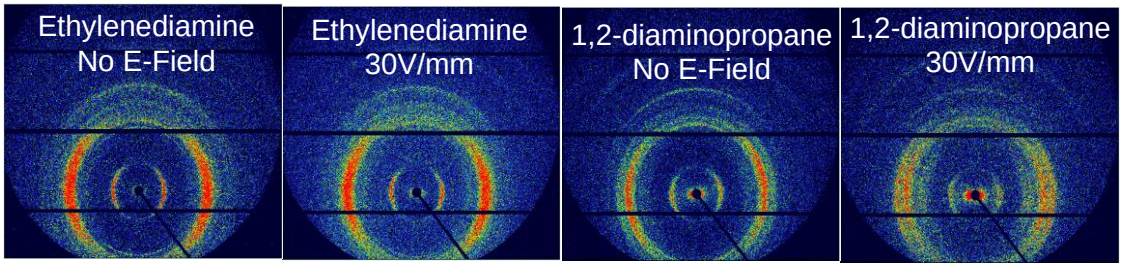

Figure 26. X-ray diffraction patterns of cotton twine after exposure to two diamines in the presence of no field or 30 V/mm.

almost nothing. However, when we aimed for 30 V/mm, the field slowly decreased to 10 V/mm over 3 hours. We designed an experiment where the twine was swelled with ethylenediamine or 1,2-diaminopropane for 2 hours, and then introduced 30 V/mm for 3 hours. After this, we dried the cotton with a nitrogen stream, yielding cellulose – amine complexes. Characterization of these samples with XRD confirmed the conversion to amine complexes, but also showed that there was no rotation of cellulose nanocrystals (Figure 26). Other experiments used methanol to wash away the diamine, but also were found to yield the amine – cellulose complexes, without any rotation. Optimally, a greater applied field would have been tried, but the distance between electrodes could not be decreased, as the twine was 1 mm wide. Also, the decrease in voltage over time was a major hurdle. We attributed the decreased voltage to a reported mechanism where ethylenediamine can coordinate to the anode, oxidize, and subsequently form linear PEI, a known insulator. After oxidation of ethylenediamine, an aziridinium ion is produced, which is opened up by nucleophilic attack from another ethylenediamine molecule (Figure 27). After this addition, there is a new free amine that can repeat this

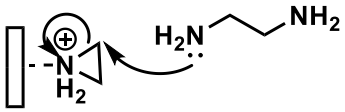

Figure 27. Proposed mechanism of formation of linear PEI.

process, which eventually results in the formation of linear PEI. Because this issue could not be circumvented, we decided to try alignment in an external magnetic field.

To do this, we needed to design a vessel in which to put vials containing both cotton and the amines. In our first attempt we introduced the cellulose to a 5 T magnetic field for five hours and subsequently tried to dry with an air stream. This resulted in the formation of salts, as diamines can react with CO_2 to form carbamates. To find a better way to remove the amines, we designed an aluminum frame with holes to allow for tubing to go into the vials. One tube was designed to remove the solvent using a syringe. Another tube was designed to introduce methanol to wash away the amine. The cotton twine was exposed to either ethylenediamine or 1,2-diaminopropane while in the presence of a 5 T field for five hours. Solvent removal and subsequent methanol introduction was repeated ten times to ensure complete removal of the amine and formation of cellulose-III, which would indicate the swelling process occurred if formed. An additional tube of air was added to evaporate the methanol overnight while still in the presence of a 5 T field. As the 1,2-diaminopropane sample was not fully dried after removal, the sample swollen with ethylenediamine was characterized to evaluate the new setup. After characterization with XRD, it was determined that even a 5 T magnetic field was not enough to rotate the cellulose nanocrystals while swollen with ethylenediamine (Figure 28). It is hypothesized that the structure of cellulose in cotton is too compact, as there are both crystalline and amorphous regions within it. It may not possible to rotate cellulose nanocrystals within the fibers in the

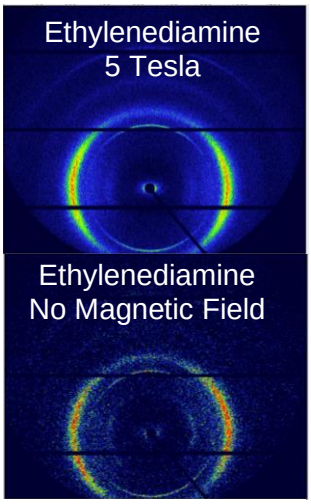

Figure 28. X-ray diffraction pattern of cellulose-III cotton twine after exposure to a 5 T magnetic field or no magnetic field.

presence of the aforementioned fields while in the swollen state. It could be useful to develop a more fundamental understanding of the process of these polymorph transformations.

Preliminary Kinetics of Cellulose-III to Cellulose-Iβ Transformation

Changes were monitored through the disappearance of peaks at 20.9, 17.1, and 11.8, which are indicative of cellulose-III. We also looked for the appearance of peaks at 22.6, 20.4, 16.3, and 14.7, which are indicative of cellulose-Iβ (Figure 29). Cellulose-III samples exposed to water at 50 °C were characterized by XRD to investigate conversion over time. After 5 minutes of exposure, the sharp peak at 17.1 is weaker and broad peaks at 16.3 and 14.7 start to form, indicating that conversion starts to take place rapidly at first.

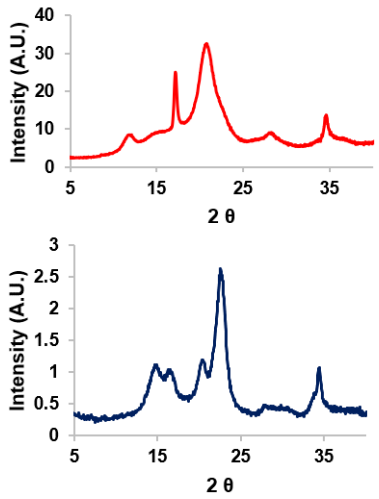

Figure 29. X-ray diffraction profiles of cellulose-III (red) and cellulose-Iβ used as standards.

After exposure to 50 °C water for 8 hours, the peak at 17.1 is diminished significantly, but still persists. Additionally, the peak at 17.1 is observed even after stirring in 50 °C water for 5 days (Figure 30).

After stirring in 80 °C water for 5 minutes, the peak at 17.1 was decreased significantly. After 8 hours, even less cellulose-III remained and after 24 hours, almost complete conversion back to cellulose-Iβ was achieved (Figure 31). These analyses are qualitative, and quantitative analysis using peak fitting software is

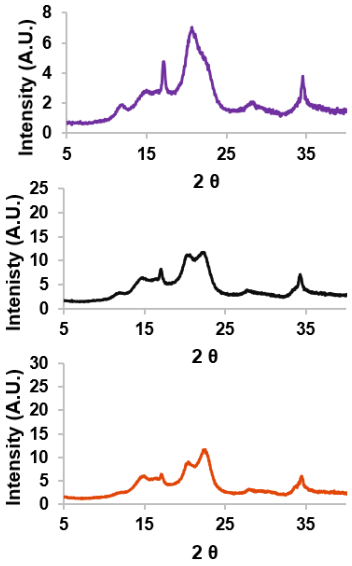

Figure 30. X-ray diffraction profiles of cellulose-III cotton balls after exposure to 50 °C H_2O for 5 minutes(purple), 8 hours (black), and 5 days (orange).

currently underway. We hope to also explore the kinetics of the transformation from the cellulose – amine complex to either cellulose-III or cellulose-Iβ.

Conclusion

The role that chain length of diamines plays in the formation of different cellulose – amine complexes was investigated with 4 new complexes being formed. The swollen states of cellulose that we used did not allow enough degrees of freedom for rotation of cellulose nanocrystals within cotton, however. To better understand cellulose polymorphs, we have just begun attempts to determine how fast the polymorph transitions take place under various conditions. We hope to more accurately quantify the transitions over time so that we can gain a better fundamental understanding of cellulose and how it is packed.

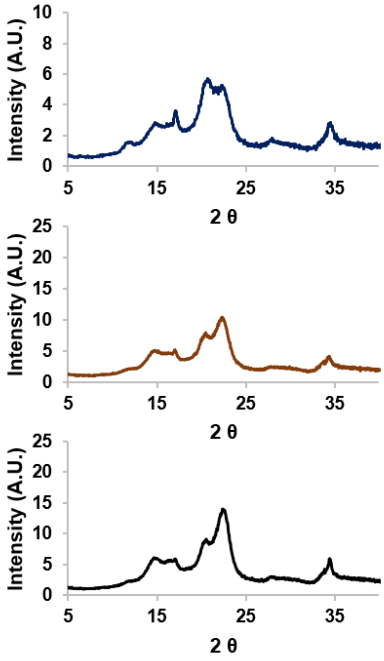

Figure 31. X-ray diffraction profiles of cellulose-III cotton balls after exposure to 80 °C H_2O for 5 minutes(blue), 8 hours (brown), and 5 days (black).

Concluding Remarks

Understanding the noncovalent interactions in natural and synthetic systems is of fundamental importance in the scientific community. As chemists, we aim at comprehending and using such supramolecular interactions to give a desired property. In this thesis, anion sensing and piezoelectricity were properties that were investigated, and drove the selection of polymers.

Chapter 2 focused on the design of a polymeric anion sensor bearing a calix[4]pyrrole-organic dye conjugate using transition-metal-catalyzed cross-coupling reactions. The two most utilized reactions in these syntheses were Sonogashira and Suzuki-Miyaura couplings. Each of these systems had their drawbacks, as a dehalogenation competed with product formation over both routes. The low yields of these reactions ultimately led to the design of a new synthetic pathway that avoided transition metal catalyzed cross-couplings.

Chapter 3 discussed a new route coupling calix[4]pyrrole to BODIPY through a Knoevenagel condensation. The phenol on BODIPY was used as a facile attachment for a polymerizable moiety. A statistical copolymer bearing this sensor side-chain along with methyl methacrylate was synthesized. This polymer was capable of binding fluoride, and also illustrated visible colorimetric and fluorometric analysis, with binding affinities on the same order of magnitude as previous calix[4]pyrrole fluoride sensors. Future work on this project could be in the tuning of polymeric properties, such as solubility in water using different comonomers, or selectivity of anion recognition using crosslinking methods.

Chapter 4 focused on natural polymers and investigated modifying the hydrogen bonding in cellulose polymorphs with diamines could be used to form other polymorphs. It was found that increasing length of diamines results in an increase spacing between cellulose chains in the swollen state. We hoped that while in this swollen state, we would be able to rotate cellulose nanocrystals within a cotton twine using an external magnetic or electric field, but were unable to achieve this. We started work on understanding the kinetic processes of the transitions between the cellulose polymorphs, and work on this is ongoing.

Integration and comprehension of the role that supramolecular chemistry can play into polymers will result in a bright future for design of materials. The crosslinking of polymers with supramolecular motifs allows for the design of materials with dynamic properties, and there is still room for creative design of new systems. Additionally, much design is still possible for motifs that can be used to bind environmental pollutants, and attachment of such motifs to polymer scaffolds enables recyclability and tunable solubility. In brief, designing polymeric materials that utilize supramolecular chemistry is a growing field that has potential to be used for a breadth of applications.

Appendix: Experimental Details

All reagents and solvents were purchased from Sigma Aldrich, Oakwood Chemical, Acros, or Beantown Chemical and used without further purification unless otherwise noted. NMR spectroscopic characterization was conducted on a Bruker Avance 500 MHz spectrometer using $CDCl_3$ unless otherwise indicated. Chemical shifts are reported in ppm, and referenced to residual $CHCl_3$. UV-visible absorption spectra were obtained on an Agilent Cary 60 UVvisible spectrophotometer (Agilent Technologies, Inc) using a quartz cuvette (Starna Cells). Fluorescence experiments were conducted using a SPEX Fluorolog 1680 spectrometer. The excitation wavelength was fixed at 590 nm and emission data was collected from 550-800 nm with 4 nm excitation and emission slit widths, 1 nm steps, and 1 sec integration time.

Meso-octamethyl calix[4]pyrrole (C4P)

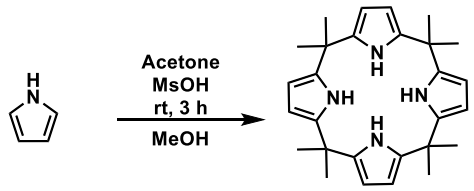

C4P

Freshly distilled pyrrole (10.5mL, 150mmol) and acetone (11.1mL, 150mmol) were combined with methanol (30mL) and stirred at 200RPM and room temperature. Catalytic amounts of methanesulfonic acid were added and the mixture was allowed to stir at 200RPM and room temperature for 3 hours. After 3 hours, all solvent was removed in

vacuo. Column chromatography (1:1 Dichloromethane:Hexanes) yielded an off white, slightly yellow product (Fraction 1, Rf = 0.45, 9.6g, 60%). ^{1}HNMR (400MHz, $CDCl_3$) δ (ppm) 1.55 (s, 24H), 5.89 (s, 8H), 6.99 (s, 4H).

Monoiodocalix[4]pyrrole (2)

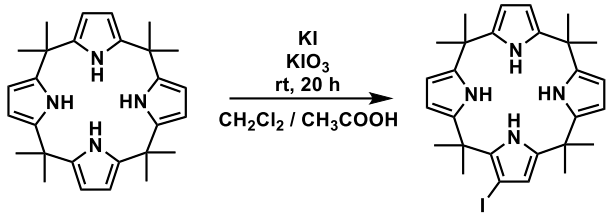

C4P **2**

Calix[4]pyrrole (7.339 g, 17.1 mmol) was dissolved in a mixture of chloroform (110 mL) and glacial acetic acid (35 mL). A homogenous mixture of potassium iodide (1.7 g, 10.2 mmol) and potassium iodate (2.2 g, 1.7 mmol) was added over the course of 3 hours. After stirring for 20 hours, the reaction mixture was washed with saturated sodium bicarbonate (5 x 30 mL) followed by brine (1 x 30 mL). The resulting organic layer was run through a plug of silica (dichloromethane) to remove any insoluble impurities. After removing the solvent in vacuo, column chromatography (1:2 dichloromethane:hexanes followed by 1:1 dichloromethane:hexanes) yielded a tan solid (2.379 g, 42 %). ^{1}HNMR (400MHz, $CDCl_3$) δ (ppm) 1.45 (s, 6H), 1.53 (s, 12 H), 1.68 (s, 6 H), 5.84-6.07 (m, 7H), 6.88 (bs, 2H), 7.21 (bs, 2H).

TMS-Acetylenecalix[4]pyrrole (3)

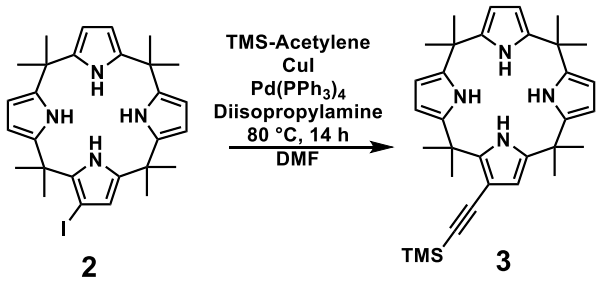

2 **3**

Monoiodocalix[4]pyrrole **2** (607 mg, 1.09 mmol) and diisopropylamine (0.45 mL, 3.1 mmol) were dissolved in DMF (15 mL). CuI (35 mg, 0.184 mmol) and $Pd(PPh_3)_4$ (75 mg, 0.064 mmol) were added and the reaction mixture was immediately sparged with nitrogen for 10 minutes. Ethynyltrimethylsilane (3.5 mL, 17 mmol) was added and the reaction mixture was sparged with nitrogen for an additional 10 minutes. Following sparging, the reaction was allowed to stir for 14 hours at 80 °C. The reaction mixture was then added to dichloromethane (60 mL), washed with brine (6 x 20 mL), and dried over Na_2SO_4. After removing the solvent in vacuo, column chromatography (3 : 1 hexane : dichloromethane followed by 1 : 1 hexane : dichloromethane) yielded a tan solid (85 mg, 15 %). ^{1}HNMR (400MHz, $CDCl_3$) δ (ppm) 0.20 (s, 9H), 1.43 (s, 6H), 1.51 (s, 12H), 1.68 (s, 6H), 5.83-6.05 (m, 7H), 6.86 (bs, 1H), 6.94 (bs, 1H), 7.14 (bs, 1H), 7.22 (bs, 1H).

Ethynylcalix[4]pyrrole (4)

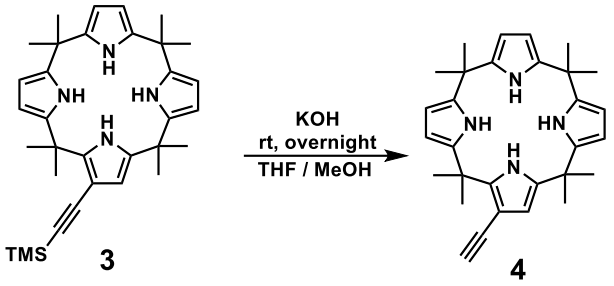

TMS-acetylenecalix[4]pyrrole **3** (144 mg, 0.287 mmol) and potassium hydroxide (190 mg, 3.4 mmol) were dissolved in methanol (1 mL) and tetrahydrofuran (2 mL) and stirred for 4 hours. The reaction mixture was then dissolved in dichloromethane (10 mL),washed with brine (3 x 5 mL), and dried over Na_2SO_4. The solvent was then removed in vacuo to yield a brown solid (130 mg, quantitative). ^{1}HNMR (400MHz, $CDCl_3$) δ (ppm) 1.47 (s, 6H), 1.54 (s, 12H), 1.70 (s, 6H), 3.10 (s, 1H), 5.86-6.07 (m, 7H), 6.85 (bs, 1H), 6.95 (bs, 1H), 7.22 (bs, 1H), 7.25 (bs, 1H).

Ethylhexyl Diketopyrrolopyrrole (DPP)

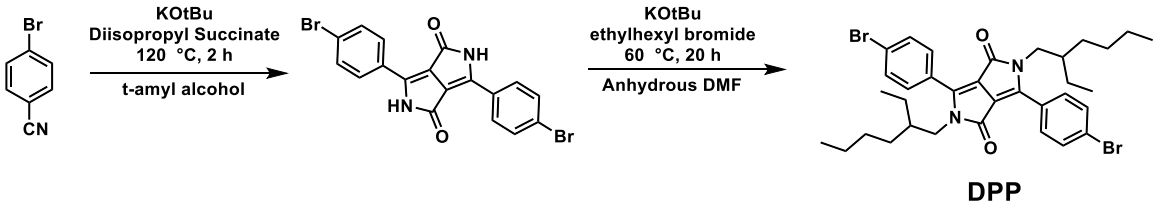

4-bromobenzonitrile (7.2 g, 39.56 mmol) and potassium tert-butoxide (5.2 g, 46.34 mmol) were dissolved in t-amyl alcohol (50 mL) and purged with nitrogen. The solution was then heated to 120 °C while stirring. Diisopropyl succinate (4 mL, 19.58 mmol) dissolved in t-amyl alcohol (10 mL) was added dropwise over the course of 1 hour and allowed to stir for an additional 2 hours at 120 °C. The mixture was cooled to 65 °C and

precipitated in a mixture of methanol (220 mL) and concentrated HCl (11 mL) and the suspension was stirred for 20 minutes. The intermediate was isolated after vacuum filtration and washed with water and methanol. The red solid intermediate was allowed to dry and then dissolved in anhydrous DMF (100 mL) along with potassium tert-butoxide (4.4 g, 39 mmol). The mixture was allowed to stir for one hour at room temperature was then heated to 60 °C while stirring. Ethylhexyl bromide (24.6 mL, 117.5 mmol) in anhydrous DMF (20 mL) was added dropwise over the course of 1 hour and the mixture was allowed to stir overnight at 60 °C. The mixture was allowed to cool to room temperature and DMF was removed in vacuo. The mixture was dissolved in ethyl acetate and washed with brine multiple times, and then dried over Na_2SO_4. Column chromatography (1 : 1 DCM : Hexanes) yielded a bright orange solid (1.2 g, 10 %). ^{1}HNMR (400MHz, $CDCl_3$) δ (ppm) 0.71 (t, 6H), 0.80 (t, 6H), 1.08-1.13 (m, 16H), 1.55 (s, 2H), 3.70-3.72 (m, 4H), 7.66 (s, 8H).

C4P-DPP Conjugate (5)

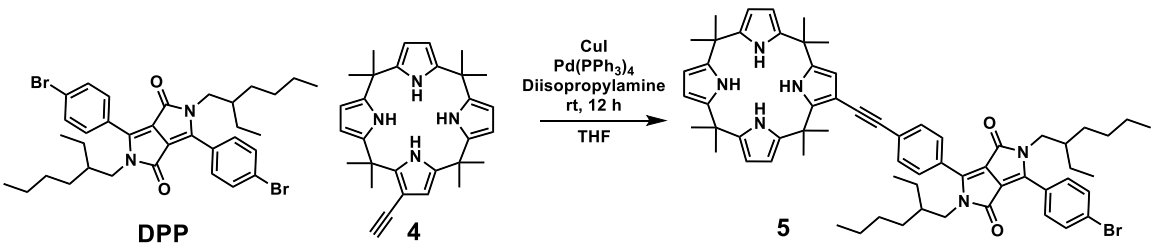

Ethynyl calix[4]pyrrole **4** (50.7 mg, 0.11 mmol) and **DPP** (130 mg, 0.21 mmol) were dissolved in THF (10 mL) and allowed to stir. The mixture was sparged with N_2 for 15 minutes. Diisopropylamine (0.2 mL, 1.4 mmol), CuI (15 mg, 0.07 mmol), and $Pd(PPh_3)_4$

(12 mg, 0.01 mmol) were added and the mixture was sparged with N_2 for 20 minutes and then allowed to stir at room temperature overnight. THF was removed in vacuo. The mixture was dissolved in DCM (20 mL) and washed with water (3 x 10 mL), 1M HCl (1 x 10 mL), and brine (1 x 10 mL), and dried over Na_2SO_4. Column chromatography (1 : 9 ethyl acetate : hexanes) yielded a bright orange solid (22 mg, 18 %). ^{1}HNMR (400MHz, $CDCl_3$) δ (ppm) 0.72 (t, 6H), 0.79 (t, 6H), 1.08-1.13 (m, 16H), 1.49 (s, 6H), 1.53 (s, 12 H), 1.55 (bs, 2H), 1.75 (s, 6H), 3.72-3.75 (m, 4H), 5.85-6.13 (m, 7H), 6.89 (bs, 2H), 7.25 (bs, 2H), 7.56 (d, 2H), 7.65 (s, 4H), 7.75 (d, 2H).

Azide Substitution of S3

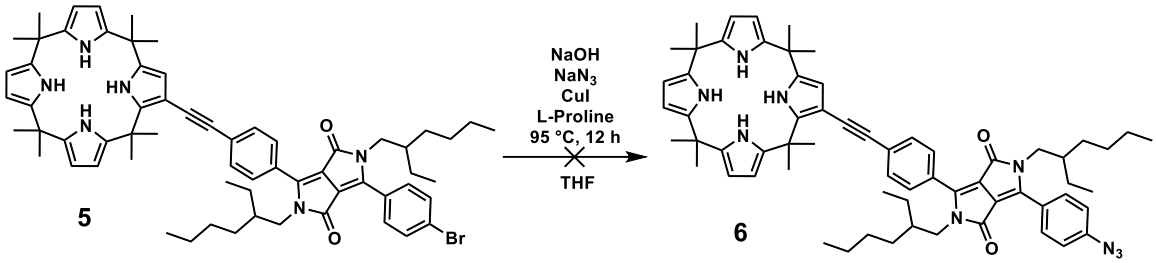

Compound **5** (5 mg, 0.0047 mmol), NaN_3 (1.4 mg, 0.0215 mmol), NaOH (0.3 mg, 0.007 mmol), CuI (cat.), and L-proline (cat.) were dissolved in THF (5 mL) and sparged with N_2 for 10 minutes. The reaction was then allowed to stir at 95 °C for 12 hours. Upon completion, what appeared to be product decomposed rapidly according to TLC and ^{1}H NMR analysis.

Compound 7

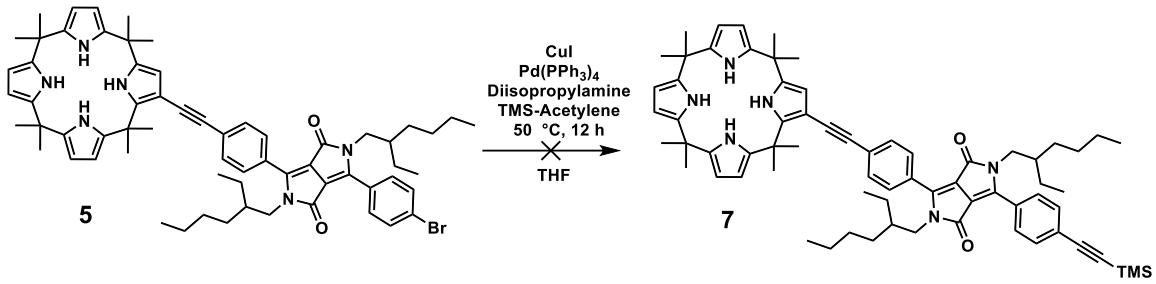

Compound **5** (50 mg, 0.048 mmol) and $Pd(PPh_3)_4$ (3 mg, 0.0025 mmol) were dissolved in THF (8 mL) and sparged with N_2 for 20 minutes. A solution of CuI (100mg, 0.52 mmol) and TMS-Acetylene (0.5 mL, 3.55 mmol) in THF (2 mL) was added to reaction mixture, and it was sparged with N_2 for 10 minutes. The mixture then stirred for 12 hours at 50 °C. Upon completion, THF was removed in vacuo. The mixture was dissolved in CH_2Cl_2 (10 mL) and washed with water (3 x 10 mL) and brine (1 x 10 mL). Preparative thin layer chromatography (2 : 1 hexanes : ethyl acetate) was used to determine contents. Starting material was recovered.

Triethylsily Pentynol

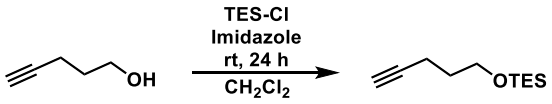

A mixture of 4-pentyn-1-ol (2 mL, 21.49 mmol), chlorotriethylsilane (7.21 mL, 42.98 mmol), and imidazole (4.39 g, 64.47 mmol) in dichloromethane (50 mL) was allowed to stir for 24 hours at room temperature. Upon completion, the mixture washed with water (3 x 30 mL) and brine (3 x 30 mL). Dichloromethane was removed in vacuo and the mixture was purified using column chromatography (hexanes to 1:1 hexanes :

DCM) to yield a clear colorless oil (2.65 g, 62 %). ^{1}HNMR (400MHz, $CDCl_3$) δ (ppm) 0.60 (q, 6H), 0.95 (t, 9H), 1.74 (d, 2H), 1.93 (s, 1H), 2.28 (m, 2H).

Compound 9

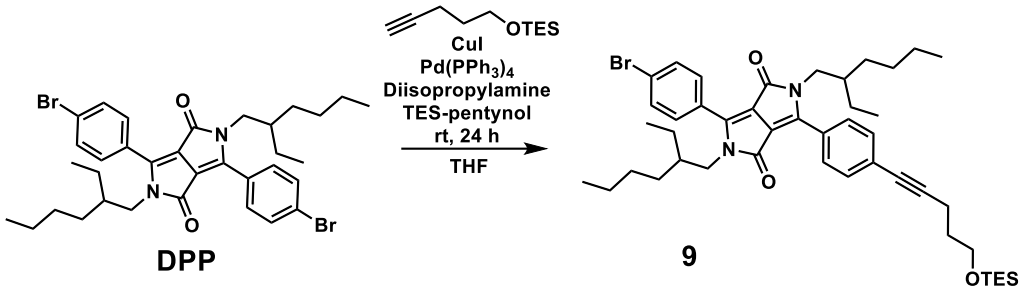

Triethylsilyl pentynol (118 mg, 0.52 mmol) and **DPP** (334 mg, 0.50 mmol) were dissolved in THF (10 mL) and the mixture was purged with a N_2 balloon three times. $Pd(PPh_3)_4$ (30 mg, 0.026 mmol) and CuI (30 mg, 0.16 mmol) was then added and the mixture was purged with a N_2 balloon three times. The reaction was then allowed to stir overnight at room temperature. Upon completion, THF was removed in vacuo and column chromatography (1 : 1 DCM : Hexanes) yielded an orange solid (59 mg, 0.075 mmoles).

Compound 10

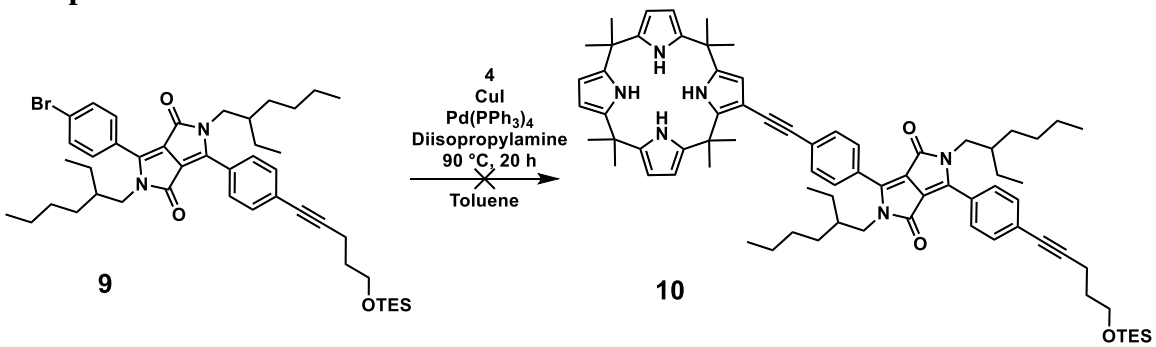

Compound **9** (59 mg, 0.075 mmol) and compound **4** (45 mg, 0.099 mmol) were dissolved in THF (10 mL). $Pd(PPh_3)_4$ (30 mg, 0.026 mmol), CuI (30 mg, 0.16 mmol), and

diisopropylamine (1 mL, 7.13 mmol) were added and the mixture was purged with a N_2 balloon three times. The mixture was stirred overnight at room temperature. Upon completion, THF was removed in vacuo and column chromatography (1:1 DCM:hexanes) yielded only starting material.

Compound 11

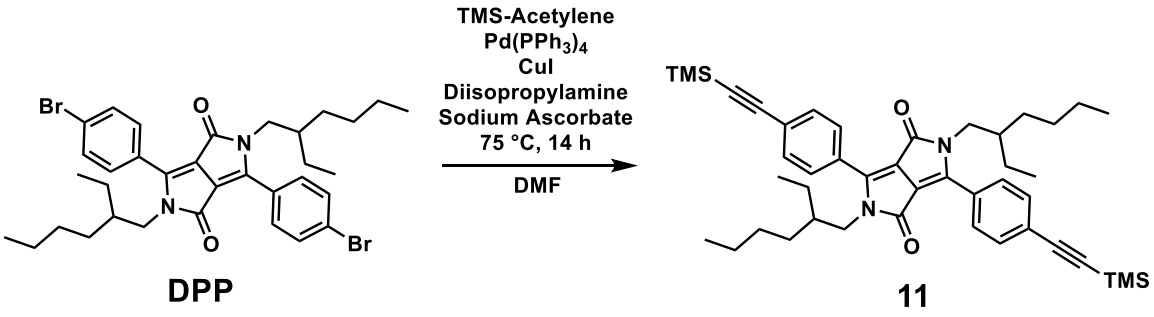

DPP (307 mg, 0.49 mmol) was dissolved in anhydrous DMF (10 mL) and sparged with N_2 for 30 minutes. Sodium ascorbate (23 mg, 0.116 mmol), CuI (9 mg, 0.048 mmol), diisopropylamine (0.2 mL, 1.5 mmol), and $Pd(PPh_3)_4$ (30 mg, 0.026 mmol) were added and the mixture was sparged with N_2 for 15 minutes. TMS-acetylene (0.11 mL, 0.73 mmol) was added while sparging, and the reaction was allowed to stir for 14 hours at 75 °C. Upon completion DMF was removed in vacuo and the mixture was dissolved in DCM (30 mL). The mixture was washed with brine (5 x 50 mL) and dried over Na_2SO_4. Column chromatography (1:1 DCM:hexanes) yielded an orange solid (87 mg, 37 %). ^{1}HNMR (400MHz, $CDCl_3$) δ (ppm) 0.26 (s, 18H), 0.69 (t, 6H), 0.79 (t, 6H), 1.07-1.18 (m, 16H), 1.46 (s, 2H), 3.72 (m, 4H), 7.57 (d, 4H), 7.73 (d, 4H). ^{13}C NMR (125 MHz, $CDCl_3$) δ (ppm) -0.11, 10.38, 13.93, 22.87, 23.67, 28.22, 30.26, 38.46, 45.12, 97.42, 104.32, 110.25, 125.80, 128.24, 128.46, 132.27, 147.96, 162.61.

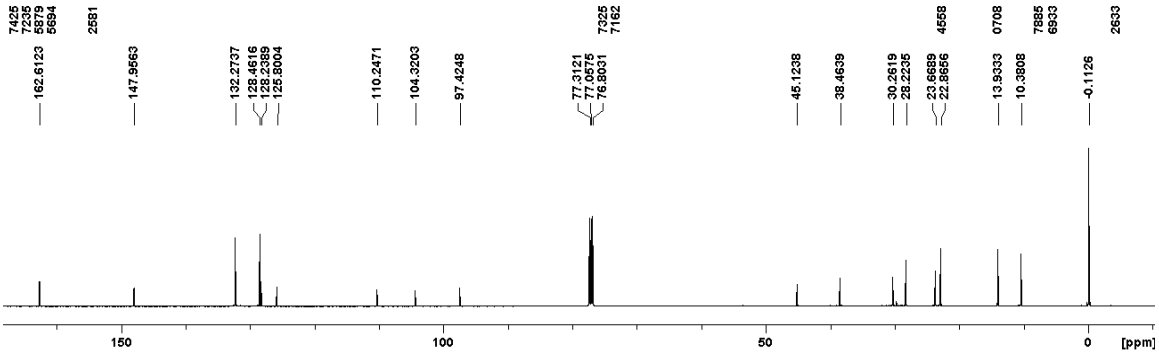

Compound 12

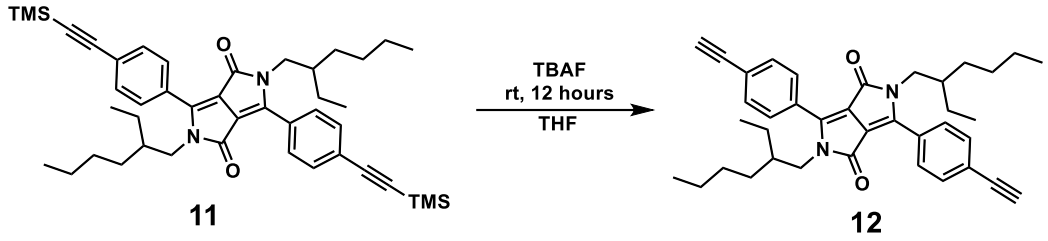

11 12

Compound **11** (47 mg, 0.072 mmol) was dissolved in THF (4 mL) and TBAF hydrate (52 mg, 0.165 mmol) was added. The mixture was allowed to stir at room temperature for 12 hours. Upon completion, THF was removed in vacuo and the mixture was dissolved in dichloromethane (10 mL). This was washed with water (3 x 10 mL) and brine (2 x 10 mL) and dried over Na_2SO_4. Column chromatography (1:1 DCM:hexanes) yielded an orange solid (14 mg, 40 %). ^{1}HNMR (400MHz, $CDCl_3$) δ (ppm) 0.71 (t, 6H), 0.79 (t, 6H), 1.08-1.16 (m, 16H), 1.46 (s, 2H), 3.23 (s, 2H), 3.73 (m, 4H), 7.62 (d, 4H), 7.75 (d, 4H).

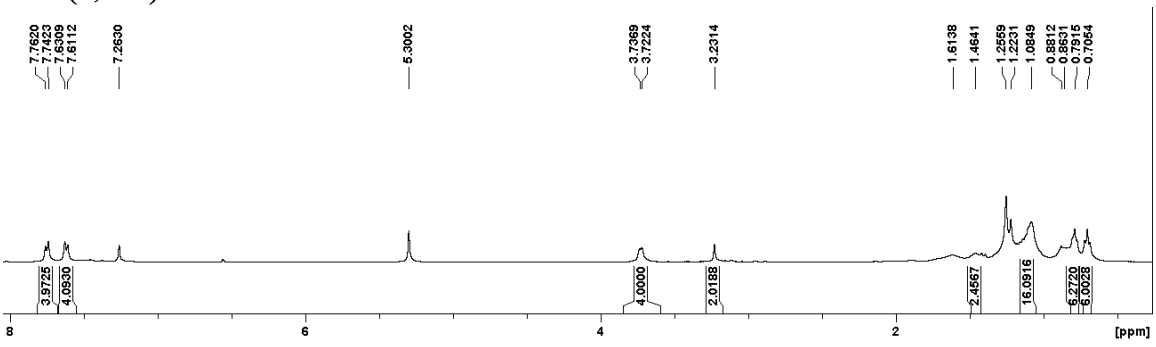

Compound 13

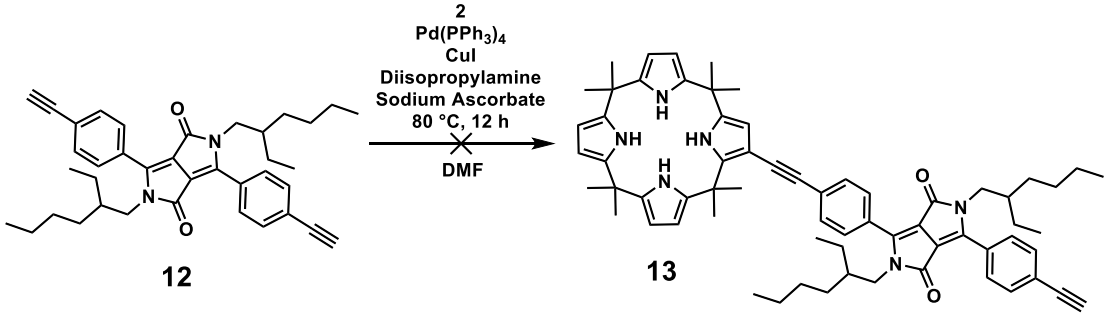

12 13

Compound **12** and compound **2** were dissolved in anhydrous DMF (5 mL) and sparged with N_2 for 10 minutes. Sodium ascorbate (1.36 mg, 0.007 mmol), CuI (1 mg, 0.005 mmol), diisopropylamine (1 mL, 7.13 mmol) and $Pd(PPh_3)_4$ (2 mg, 0.0017 mmol) were then added and the mixture was sparged with N_2 for 15 minutes. The mixture was allowed to stir at 80 °C for 12 hours. Upon completion, column chromatography (1:1 DCM:hexanes) yielded only compound **12** and dehalogenated **C4P**.

Ethylhydroxycalix[4]pyrrole (14)

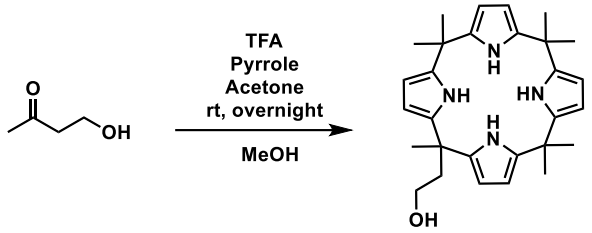

14

Freshly distilled pyrrole (15.7 mL, 226.8 mmol), acetone (12.48 mL, 170 mmol), and 4-hydroxy-2-butanone (4.88 mL, 56.7 mmol) were dissolved in methanol (650 mL) and began stirring. Trifluoroacetic acid (2 mL, catalytic) was added dropwise and the mixture was allowed to stir at room temperature overnight. Upon completion, methanol was removed in vacuo and the mixture was run through a plug of silica (dichloromethane). Column chromatography (dry load, 3:1 DCM:hexanes to 3:1 hexanes:ethyl acetate) yielded a tan solid (Rf in 3:1 hexanes:ethyl acetate = 0.5, 4.671 g, 18 %). ^{1}HNMR (400MHz, $CDCl_3$) δ (ppm) 1.49 (s, 21H), 2.14 (t, 2H), 3.59 (t, 2H), 5.89 (s, 8H), 6.98 (bs, 2H), 7.06 (bs, 2H).

TBDMS-Ethylhydroxycalix[4]pyrrole (15)

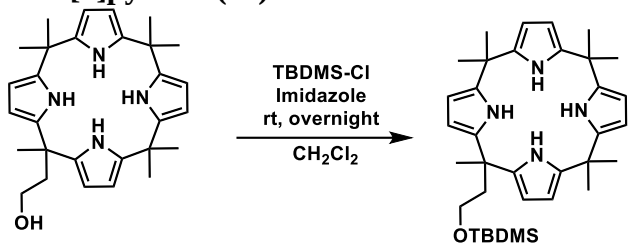

14 **15**

Ethylhydroxy calixpyrrole (500 mg, 1.09 mmol), TBDMS-Cl (181 mg, 1.2 mmol), and imidazole (165 mg, 2.4 mmol) were dissolved in CH_2Cl_2 (15 mL) and allowed to stir at room temperature for 14 hours. Upon completion, dichloromethane was removed in vacuo and column chromatography (2:1 DCM:hexanes) yielded a tan solid (579 mg, 89 %). ^{1}HNMR (500MHz, $CDCl_3$) δ (ppm) -0.02 (s, 6H), 0.85 (s, 9H), 1.49-1.51 (m, 21H), 2.12 (t, 2H), 3.46 (t, 2H), 5.90 (s, 8H), 6.98 (bs, 4H). ^{13}C NMR (125 MHz, $CDCl_3$) δ (ppm) -5.26, 18.32, 25.98, 26.65, 29.06, 35.20, 37.46, 42.95, 60.07, 102.85, 103.88, 136.90, 138.41, 138.47, 138.60.

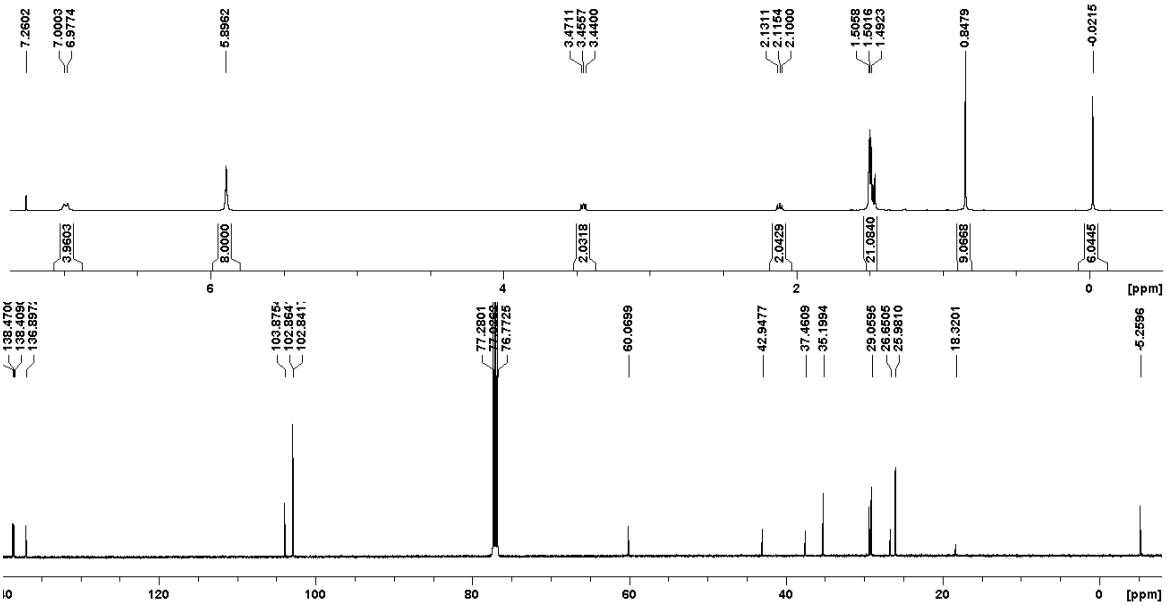

Iodinated-TBDMS-Ethylhydroxycalix[4]pyrrole (16)

Compound **15** (1.183 g, 2.06 mmol) was dissolved in a mixture of $CHCl_3$ (14 mL) and glacial CH_3COOH (4 mL) and allowed to stir. A homogeneous solid mixture of KI

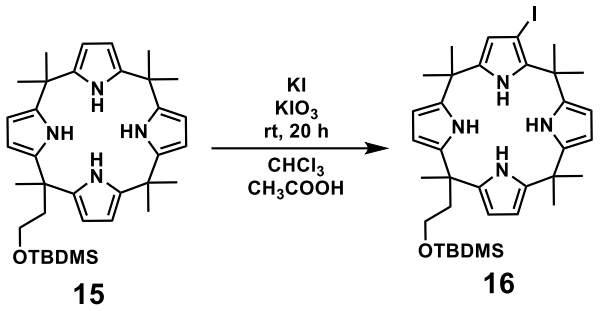

15 **16**

(204 mg, 1.23 mmol) and KIO_3 (264 mg, 1.23 mmol) was added to the mixture over the course of 3 hours and then allowed to stir for 20 hours at room temperature. Upon completion, the mixture was washed with $NaHCO_3$ (5 x 30 mL) and brine (1 x 30 mL). The mixture was run through a plug of silica (dichloromethane) and then then column chromatography (1:1 DCM:hexanes) yielded a tan solid (450 mg, 52 %). ^{1}HNMR (500MHz, $CDCl_3$) δ (ppm) 0.02 (s, 6H), 0.87 (s, 9H), 1.48 (m, 6H), 1.54 (m, 10H), 1.71 (m, 5H), 2.17 (t, 2H), 3.52 (m, 2H), 5.86-6.11 (m, 7H), 6.93 (bs, 2H), 7.25 (bs, 2H). HRMS:

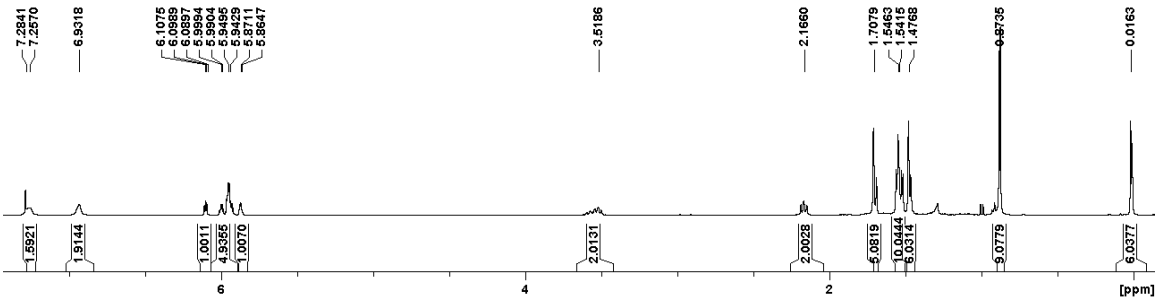

699 [M + Na] calculated, 699 found.

Monobrominated diketopyrrolopyrrole (18)

Benzonitrile (6.5 mL, 63 mmol), 4-bromobenzonitrile (10.92 g, 60 mmol), and

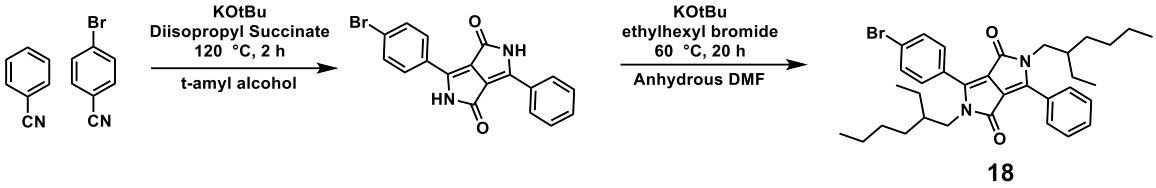

18

potassium tert-butoxide (15.48 g, 138 mmol) were added to t-amyl alcohol (100 mL) and began stirring. The mixture was heated to 120 °C and a mixture of diisopropyl succinate (7.02 mL, 48 mmol) in t-amyl alcohol (10 mL) was added dropwise over the course of 1 hour. After addition, the mixture was allowed to stir at 120 °C for 3 hours. After 3 hours, the mixture was cooled to 65 °C and then precipitated into a mixture of methanol (200 mL) and concentrated HCl (30 mL). The solid was filtered and washed with water (2x 100 mL) and methanol (2 x 100 mL) and allowed to dry. The red precipitate (13.04 g) was then dissolved in anhydrous DMF (170 mL). Potassium tert-butoxide (8 g, 71 mmol) was then added and the mixture was heated to 60 °C. Ethylhexyl bromide (31.3 mL, 176 mmol) in DMF (30 mL) was then added dropwise over the course of 1 hour. The mixture was then stirred at 60 °C for 20 hours. Upon completion, the mixture was run through a plug of silica (dichloromethane) and column chromatography (2:1 DCM:hexanes) yielded an orange solid (339 mg, 3 % over 2 steps). ^{1}HNMR (500MHz, $CDCl_3$) δ (ppm) 0.70 (m, 6H), 0.77 (m, 6H), 1.02-1.22 (m, 16H), 1.45 (s, 2H), 3.71 (m, 4H), 7.49 (m, 3H), 7.63 (d, 4H), 7.73 (m, 2H). ^{13}C NMR (125 MHz, $CDCl_3$) δ (ppm) 10.36, 10.42, 13.94, 22.82, 22.86, 23.70,

23.73, 28.24, 30.29, 38.49, 38.54, 44.91, 109.60, 110.04, 125.40, 127.42, 128.43, 128.63, 128.83, 130.08, 130.99, 132.12, 147.18, 149.25, 162.56, 162.70.

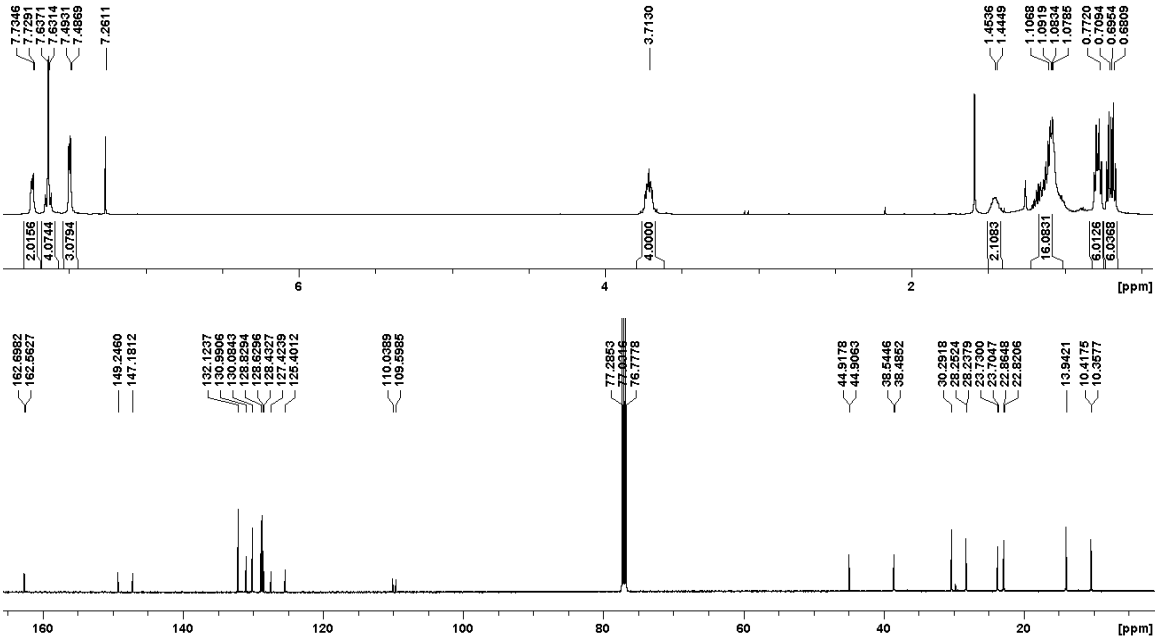

Monoborylated diketopyrrolopyrrole (19)

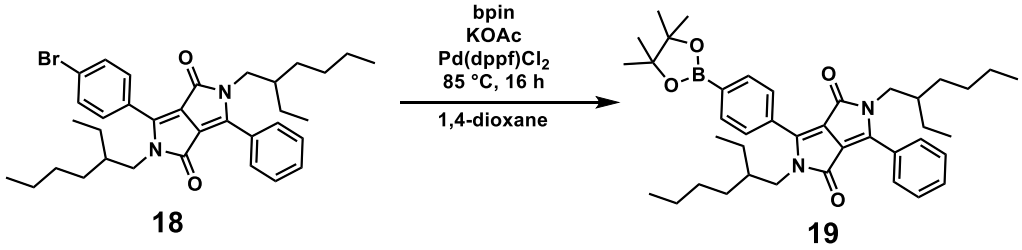

18 **19**

Compound **18** (261 mg, 0.441 mmol) was added to 1,4-dioxane (4 mL) and began stirring. Potassium acetate (473 mg, 4.82 mmol), bis(pinacolato)diboron (125 mg, 0.482 mmol), and Pd(ddpf)Cl_2 (35 mg, 0.0484 mmol) were added and the mixture was sparged with N_2 for 10 minutes. The mixture was then allowed to stir at 85 °C for 16 hours. Upon completion, 1,4-dioxane was removed in vacuo and column chromatography (dichloromethane) yielded a bright orange solid (229 mg, 81 %). ^{1}HNMR (500MHz,

$CDCl_3$) δ (ppm) 0.68 (m, 6H), 0.76 (m, 6H), 1.03-1.18 (m, 16H), 1.36 (s, 12H), 1.47 (s, 2H), 3.72 (M, 4h), 7.50 (m, 3H), 7.74 (dd, 4H), 7.93 (d, 2H). ^{13}C NMR (125 MHz, $CDCl_3$) δ (ppm) 10.36, 10.41, 13.95, 22.82, 22.85, 23.70, 24.86, 24.88, 28.23, 29.71, 30.29, 38.45, 38.51, 44.88, 45.01, 84.12, 109.78, 110.10, 127.69, 128.63, 128.82, 130.92, 131.01, 148.44, 149.02, 162.72.

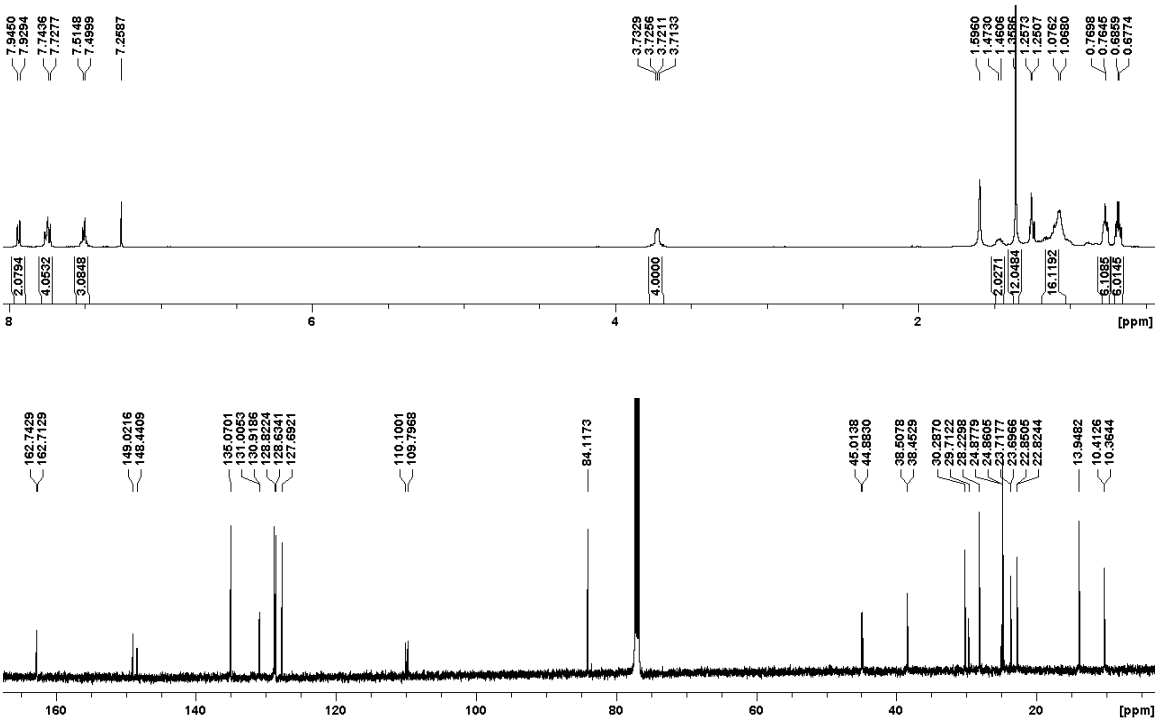

Suzuki-Miyaura Coupling (20)

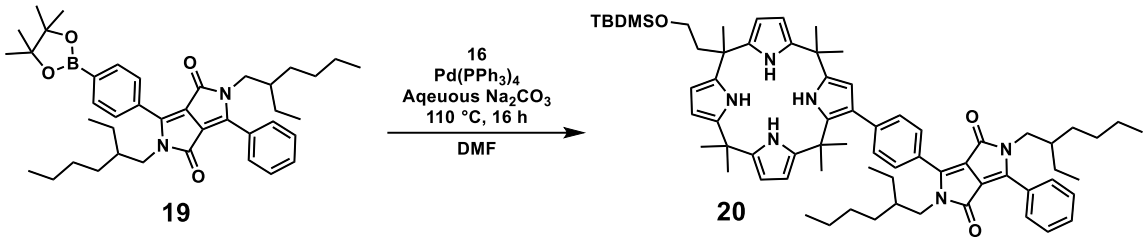

Compound **19** (95 mg, 0.161 mmol) and compound **16** (113 mg, 0.161 mmol) were dissolved in anhydrous DMF (4 mL) and sparged with N_2 for 10 minutes. Na_2CO_3 (148 mg, 1.4 mmol) in a minimal amount of water was then added and the mixture was allowed to stir for 12 hours at 110 °C. Column chromatography (9:1 hexanes : ethyl acetetate to 7:1 hexanes : ethyl acetate) yielded an orange solid (14 mg, 7 %). ^{1}HNMR (500MHz, $CDCl_3$) δ (ppm) -0.01 (m, 6H), 0.69-0.77 (m, 12H), 0.85 (m, 9H), 1.06-1.19 (m, 16H), 1.51 (m, 6H), 1.55 (s, 16H), 2.14 (m, 2H), 3.47 (m, 2H), 3.75 (m, 4H), 5.84-6.11 (m, 7H), 7.03 (bs, 2H), 7.19 (bs, 2H), 7.50 (m, 5H), 7.76 (m, 4H). HRMS: 1117 [M + Na] calculated, 1117.7 found.

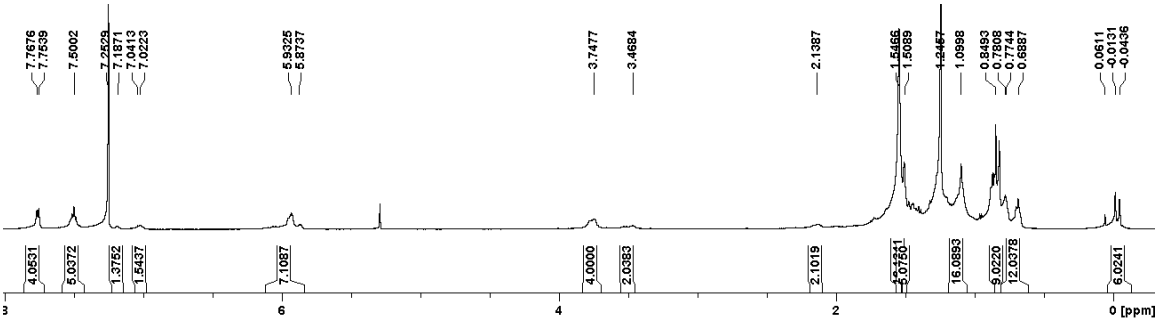

TBAF Deprotection (21)

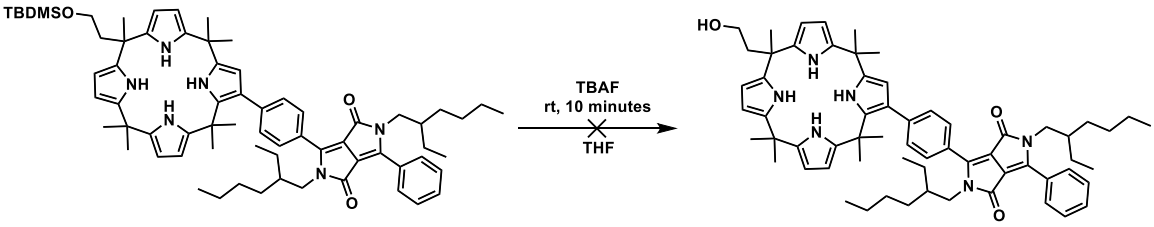

Compound **20** (5 mg, 0.0043 mmol) was dissolved in THF (3 mL) and began stirring. TBAF (0.1mL 1M solution in THF) was added and the mixture was allowed to stir for 5 minutes. Upon addition, the reaction mixture changed from a bright yellow to a colorless solution. Fluoride decomposed the dye.

Mitsunobu Reaction (22)

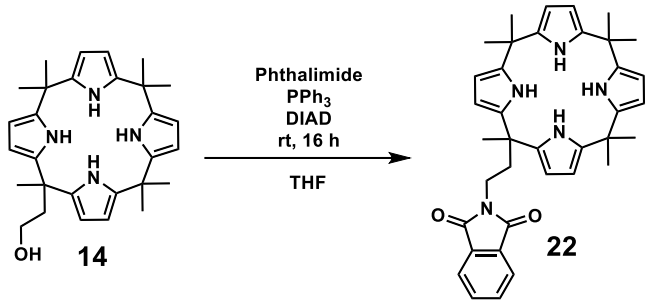

Compound **14** (1.117 g, 2.43 mmol), phthalimide (430 mg, 2.92 mmol), PPh_3 (766 mg, 2.92 mmol), and diisopropyl azodicarboxylate (0.61 mL, 2.92 mmol) were dissolved in anhydrous THF (40 mL) and the mixture was sparged with N_2 for 10 minutes. The mixture was then allowed to stir at room temperature overnight. Upon completion, THF was removed in vacuo and column chromatography (9:1 hexane : hexanes : ethyl acetate to 4:1 hexane : ethyl acetate) yielded a bright yellow solid (1.253 g, 88 %). ^{1}HNMR (500MHz, $CDCl_3$) δ (ppm) 1.47 (s, 3H), 1.50 (m, 8H), 1.54 (s, 8H), 1.58 (s, 2H), 2.22 (t,

2H), 3.54 (t, 2H), 5.83-5.92 (m, 8H), 7.07 (bs, 2H), 7.16 (bs, 2H), 7.67 (d, 2H), 7.78 (d, 2H).

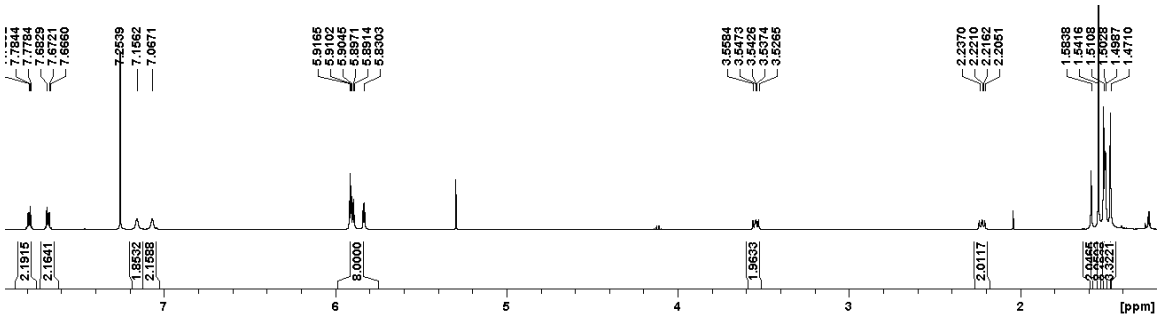

Dipyrromethane (24)

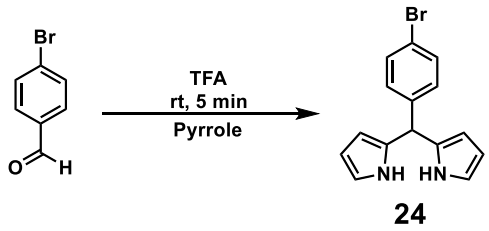

24

To freshly distilled pyrrole (125 mL, 1800 mmol) was added 4-bromobenzaldehde (6.5 g, 36 mmol) and then allowed to stir at room temperature for 10 minutes. Trifluoroacetic acid (0.28 mL, 3.6 mmol) was added and the reaction mixture was allowed to stir for 5 minutes. During this time, the mixture turned brown. After 5 minutes, KOH (1M, 60 mL) was added and the reaction mixture turned yellow. The mixture was then dissolved in diethyl ether and washed with water (1 x 200 mL) and brine (1 x 200 mL). The mixture was then run through a plug of silica (dichloromethane) and evaporated to obtain an oil. A small amount of dichloromethane was added (< 5 mL) to break up the oil. Upon addition of hexanes (~ 15 mL), a precipitate formed to obtain a brown solid (10.194 g, 94 %). ^{1}HNMR (400MHz, $CDCl_3$) δ (ppm) 5.41 (s, 1H), 5.95 (s, 2H), 6.25 (q, 2H), 6.43 (q, 1H), 7.12 (d, 2H), 7.50 (d, 2H), 7.81 (bs, 2H).

BODIPYlation (25)

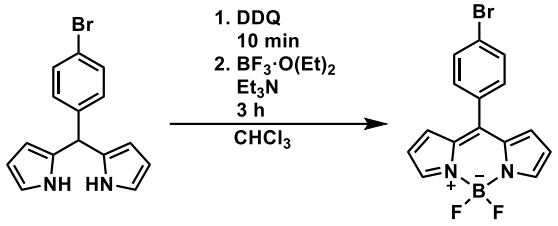

24 **25**

Dipyrromethane **24** (1.20 g, 4 mmol) was dissolved in CH_2Cl_2 (100 mL) and cooled to 0 °C. DDQ (908 mg, 4 mmol) was added and the mixture was allowed to stir for 10 minutes. Triethylamine (8 mL, 57.3 mmol) was added immediately followed by a dropwise addition of boron trifluoride diethyletherate (8 mL, 64.8 mmol). After addition, the mixture was allowed to warm to room temperature and stir for 3 hours. CH_2Cl_2 was removed in vacuo and the mixture was run through a plug of silica (dichloromethane). Column chromatography (2:1 DCM:hexanes) yielded a red solid (314 mg, 23 %). ^{1}HNMR (400MHz, $CDCl_3$) δ (ppm) 6.57 (d, 2H), 6.91 (d, 2H), 7.44 (d, 2H), 7.68 (d, 2H), 7.96 (s, 2H).

Borylation (26)

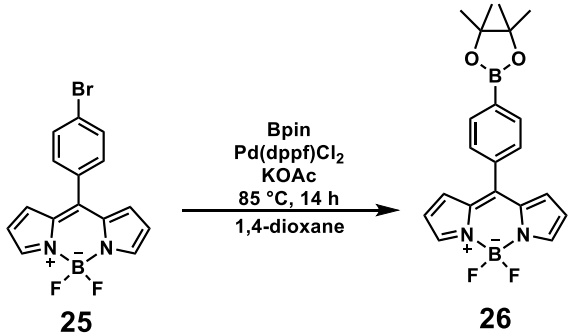

25 **26**

Compound **25** (566 mg, 1.63 mmol), potassium acetate (800 mg, 8.15 mmol), bis(pinacolato)diboron (414 mg, 1.63 mmol), and $Pd(dppf)Cl_2$ (119 mg, 0.163 mmol) were dissolved in 1,4-dioxane (10 mL) and sparged with N_2 for 10 minutes. The reaction mixture was then heated to 85 °C and allowed to stir for 14 hours. Upon completion, 1,4-dioxane was removed in vacuo and column chromatography (dichloromethane) yielded a bright orange solid (327 mg, 51 %). ^{1}HNMR (500MHz, $CDCl_3$) δ (ppm) 1.38 (s, 12H), 6.53 (d, 2H), 6.91 (d, 2H), 7.55 (d, 2H), 7.95 (m, 4H).

Suzuki Coupling (27)

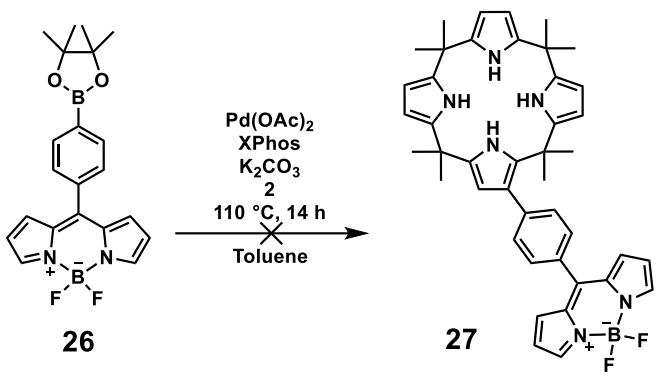

26 **27**

Compound **26** (240 mg, 0.61 mmol) and compound **2** (169 mg, 0.305 mmol) were dissolved in toluene (10 mL) and allowed to stir. XPhos (10 mg, 0.021 mmol) and $Pd(OAc)_2$ (3 mg, 0.013 mmol) were then added, followed by K_2CO_3 (88 mg, 0.64 mmol). The reaction mixture was then sparged with N_2 for 10 minutes and allowed to stir for 14 hours at 100 °C. Upon completion, toluene was removed in vacuo and column chromatography (1:1 DCM:hexanes) yielded mostly comound **26**, as well as dehalogenated calixpyrrole and deborylated BODIPY.

BODIPY (29)

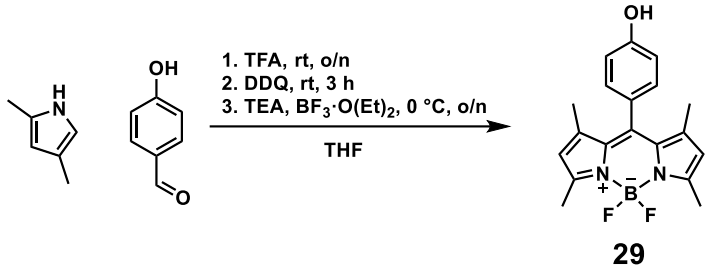

29

To 75 mL of anhydrous THF was added 2,4-dimethypyrrole (1.0 mL, 9.7 mmol) and 4-hydroxybenzaldehyde (593 mg, 4.85 mmol). After stirring the reaction mixture for 5 minutes, 3 drops of trifluoroacetic acid were added and the reaction mixture was allowed to stir overnight. After consumption of 4-hydroxybenzaldehyde as determined by TLC, 2,3-Dichloro-5,6-dicyano-1,4-benzoquinone (1.1 g, 4.85 mmol) dissolved in 75 mL anhydrous THF was added dropwise over the course of 10 minutes and upon addition allowed to stir for 3 hours at room temperature. The reaction mixture was cooled to 0 °C and 25 mL of triethylamine (179 mmol) was added. The reaction mixture was allowed to stir for 20 minutes before 25 mL boron trifluoride diethyletherate (202 mmol) was added dropwise over the course of 15 minutes. The reaction mixture was then allowed to stir overnight. THF was removed in vacuo the next day. The reaction mixture was dissolved in DCM and subsequently washed with water multiple times, followed by saturated $NaHCO_3$ (x2) and brine (x2) and dried over Na_2SO_4. The product was purified using column chromatography (2:1 hexanes : ethyl acetate) to yield a dark red solid (Rf = 0.5, 517 mg, 31 %). ^1H NMR (500 MHz, $CDCl_3$) δ (ppm) 1.44 (s, 6H), 2.55 (s, 6H), 4.97 (s, 1H), 5.97 (s, 2H), 6.95 (d, 2H), 7.12 (d, 2H).

TBDMS Protected BODIPY (30)

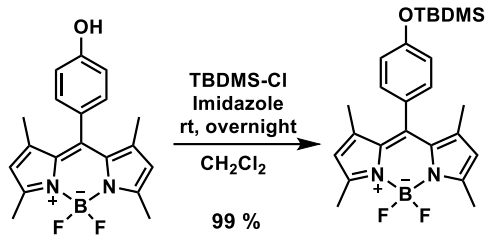

29 **30**

BODIPY **29** (43 mg, 0.126 mmol), imidazole (22 mg, 0.319 mmol), and tert-butyldimethylsilyl chloride (21 mg, 0.139 mmol) were dissolved in DCM (10 mL) and allowed to stir overnight. The next day the solvent was removed in vacuo and purified with column chromatography (1:9 ethyl acetate : hexanes) to yield a bright orange solid (first band, 57 mg, 99 %). ^{1}H NMR (500 MHz, $CDCl_3$) δ (ppm) 0.21 (s, 6H), 1.00 (s, 9H), 1.43 (s, 6H), 2.54 (s, 6H), 5.97 (s, 2H), 6.97 (d, 2H), 7.10 (d, 2H). ^{13}C NMR (125 MHz, $CDCl_3$) δ (ppm) -4.43, 1.05, 14.43, 18.36, 25.69, 29.73, 121.12, 127.95, 129.19, 131.76, 141.92, 143.13, 155.25, 156.45. LCMS: 455 [M + H] calculated, 455.3 found. 487 [M + Na] calculated, 487.3 found.

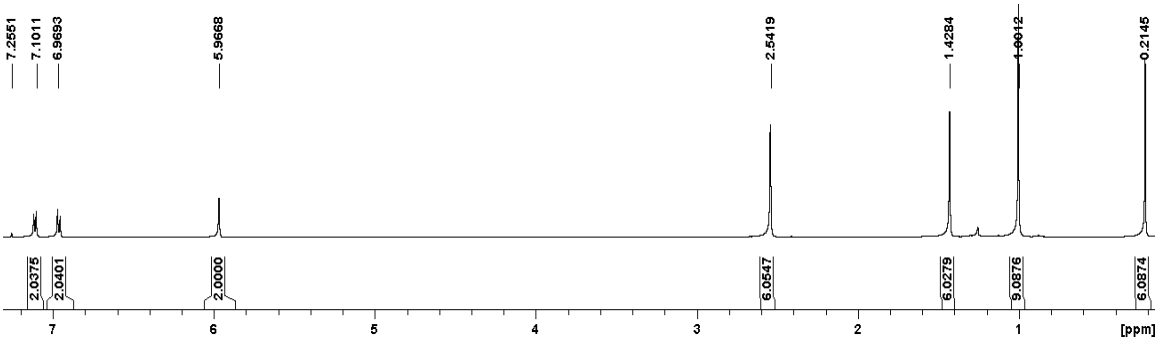

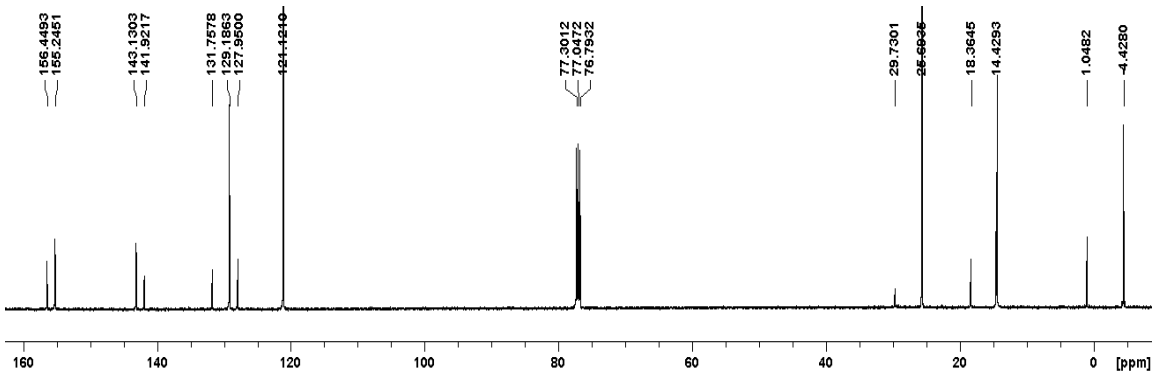

Formyloctamethylcalix[4]pyrrole (31)

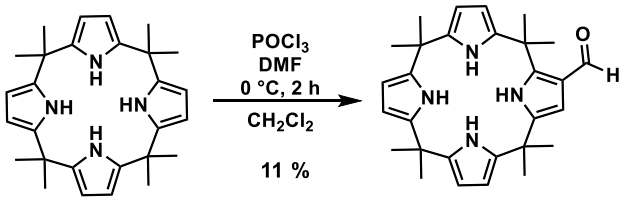

C4P **31**

To anhydrous DCM (2.5 mL) was added $POCl_3$ (0.26 mL, 2.79 mmol) and anhydrous DMF (0.22 mL, 2.79 mmol) and stirred for 30 minutes. This mixture was then added dropwise to a 0 °C solution of octamethylcalix[4]pyrrole (1.20 g, 2.79 mmol), in anhydrous DCM (50 mL). This was allowed to stir for 2 hours and then washed with saturated $NaHCO_3$ (2x) and brine (2x). The solvent was removed in vacuo and column chromatography (2 % methanol in DCM) yielded the second fraction as a tan solid (Rf = 0.5, 139 mg, 11 %). ^{1}H NMR (400MHz, $CDCl_3$) δ (ppm) 1.48 (s, 6H), 1.53 (s, 12 H), 1.72 (s, 6H), 5.80-6.00 (m, 6H), 6.43 (d, 1H), 7.02 (bs, 1H), 7.25 (bs, 1H), 7.46 (bs, 1H), 7.51 (bs, 1H), 10.04 (s, 1H).

Knoevenagel condensation product (32)

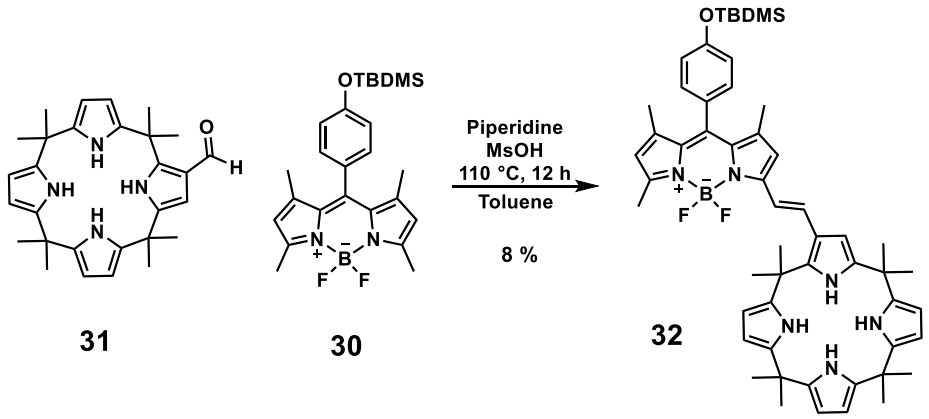

Compound **3** (498 mg, 1.09 mmol) and compound **4** (568 mg, 1.24 mmol) were dissolved 100 mL toluene equipped with molecular sieves and a Dean-Stark trap. Piperidine (2.67 mL, 27 mmol) and a catalytic amount of methanesulfonic acid were added to the reaction mixture. The mixture was then stirred for 14 hours at 110 °C. The next day the solvent was removed in vacuo and purified via column chromatography (3:1 DCM : hexanes). The second fraction (purple) was collected to yield a purple solid (79 mg, 8 %). ^{1}H NMR (500 MHz, $CDCl_3$) δ (ppm) 0.22 (s, 6H), 1.01 (s, 9H), 1.44 (s, 3H), 1.48 (s, 3H), 1.52-1.55 (m, 18H), 1.68 (s, 6H), 2.59, (s, 3H), 5.86-5.96 (m, 7H), 6.39 (bs, 1H), 6.49 (s, 1H), 6.88 (bs, 2H), 6.96 (d, 2H), 7.15 (m, 3H), 7.20 (bs, 1H), 7.24 (bs, 1H), 7.60 (d, 1H). ^{13}C NMR (125 MHz, $CDCl_3$) δ (ppm) -4.42, 14.16, 14.22, 14.30, 14.61, 14.77, 18.36, 22.72, 25,70, 28.66, 28.70, 29.35, 29.73, 31.95, 35.11, 35.20, 35.26, 37.37, 101.84, 102.87,

103.03, 103.15, 103.60, 103.74, 103.84, 114.74, 117.34, 120.35, 120.98, 128.38, 129.60, 131.68, 137.30, 137.32, 137.64, 138.13, 138.33, 139.14, 139.30, 140.64 155.26, 156.34.

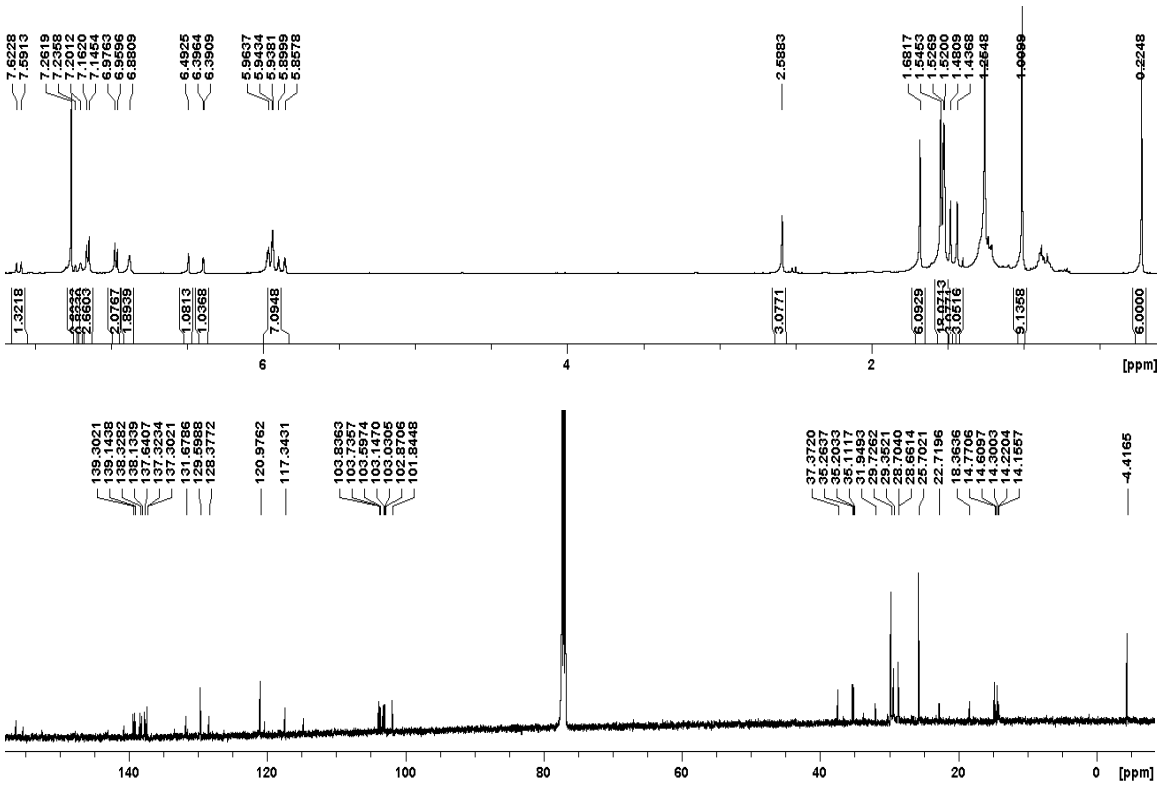

Deprotection of TBDMS ether to form (33)

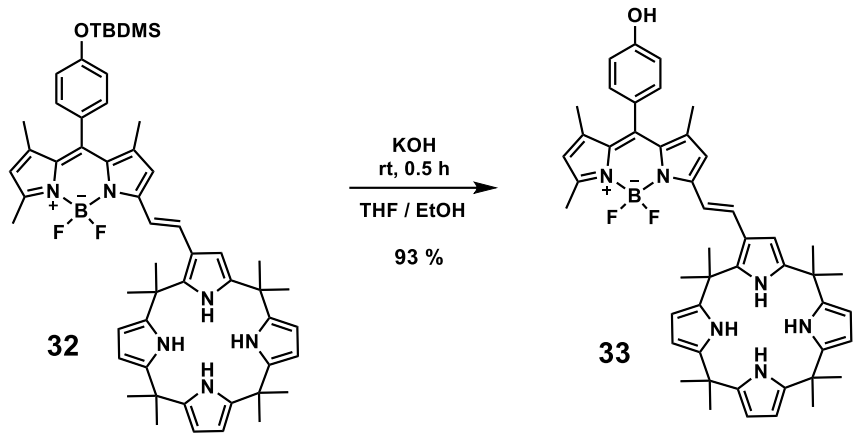

Compound **32** (79 mg, 0.088 mmol) was dissolved in a mixture of THF (4 mL) and ethanol (1 mL) and began stirring. Potassium hydroxide (7.5 mg, 0.133 mmol) was added using 1 mL of a stock solution of KOH in ethanol, and the reaction was stirred for 30 minutes. After completion by TLC, the solvent was removed in vacuo, and the mixture was purified using column chromatography (5 % ethyl acetate in DCM) to yield a purple solid (64 mg, 93 %). ^{1}H NMR (500 MHz, $CDCl_3$) δ (ppm) 1.45 (s, 3H), 1.49 (s, 3H), 1.53-1.60 (m, 18H), 1.68 (s, 6H), 2.59 (s, 3H), 5.86-6.05 (m, 7H), 6.40 (s, 1H), 6.50 (s, 1H), 6.90 (bs, 2H), 6.94 (d, 2H), 7.16 (m, 3H), 7.24, (bs, 1H), 7.32 (bs, 1H) 7.60 (d, 1H). ^{13}C NMR (125 MHz, $CDCl_3$) δ (ppm) 14.15,14.46, 14.95, 22.72, 23.33, 24.69, 28.68, 28.72, 29.37, 29.72, 31.95, 35.12, 35.22, 35.27, 36.63, 37.37, 101.79, 102.86, 103.05, 103.15, 103.72, 103.85, 116.00,117.42, 120.32, 127.79, 129.85, 131.79, 137.35, 137.73, 138.05, 138.15, 138.46, 139.26, 139.36, 156.05.

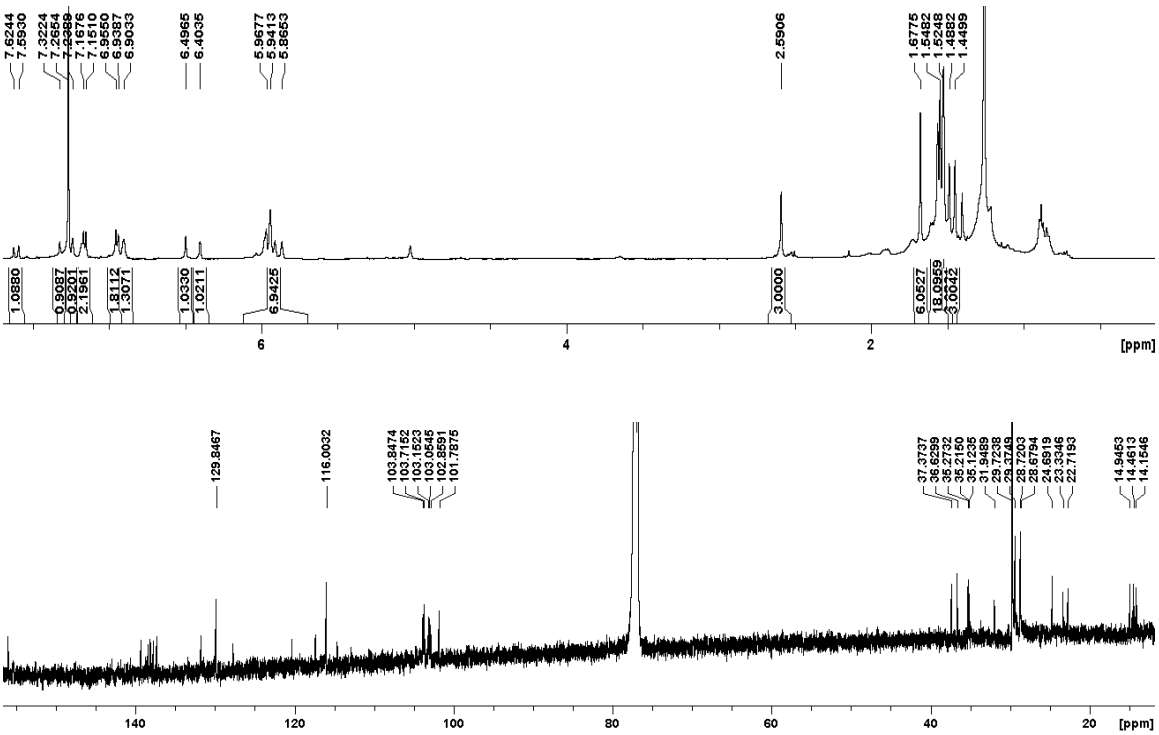

Acyl substitution onto methacryloyl chloride to form (34)

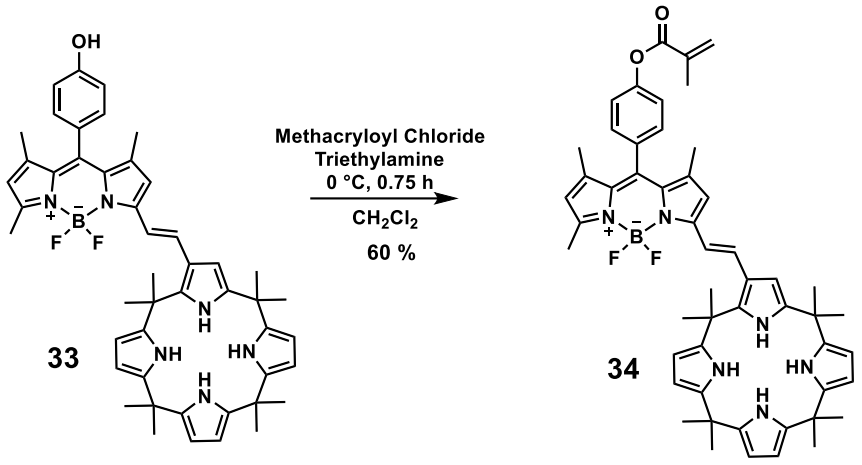

Compound **33** (64 mg, 0.082 mmol) was dissolved anhydrous DCM (3 mL) and cooled to 0 °C while stirring. Triethylamine (0.014 mL, 0.1 mmol) was added followed by methacryloyl chloride (0.01 mL, 0.1 mmol) and the reaction stirred for 45 minutes. Note:

triethylamine and methacryloyl chloride were added using stock solutions in anhydrous DCM to give a total volume of 4 mL for the reaction mixture. Upon completion by TLC, the solvent was removed in vacuo and the mixture was purified by column chromatography (DCM) to yield an indigo colored solid (42 mg, 60 %). ^{1}H NMR (500 MHz, $CDCl_3$) δ (ppm) 1.44 (s, 3H), 1.49 (s, 3H), 1.52-1.54 (m, 18H), 1.68 (s, 6H), 2.09 (s, 3H), 2.59 (s, 3H), 5.80 (s, 1H), 5.86-5.97 (m, 7H), 6.40 (bs, 2H), 6.52 (s, 1H), 6.93 (bs, 2H), 7.21 (bs, 1H), 7.26 (m, 4H), 7.35 (d, 2H), 7.62 (d, 1H). ^{13}C NMR (125 MHz, $CDCl_3$) δ (ppm) 7.96, 14.46, 14.63, 14.93, 18.42, 23.38, 24.71, 28.70, 28.75, 29.39, 29.79, 35.14, 35.23, 35.29, 36.65, 37.41, 101.81, 102.85, 103.05, 103.18, 103.64, 103.71, 103.86, 114.52, 117.33, 117.68, 120.49, 122.49, 125.80, 126.04, 127.69, 128.93, 129.60, 132.18, 132.88, 135.68, 137.32, 137.37, 137.70, 138.09, 138.21, 138.66, 139.24, 139.39, 140.52, 142.94, 151.38,

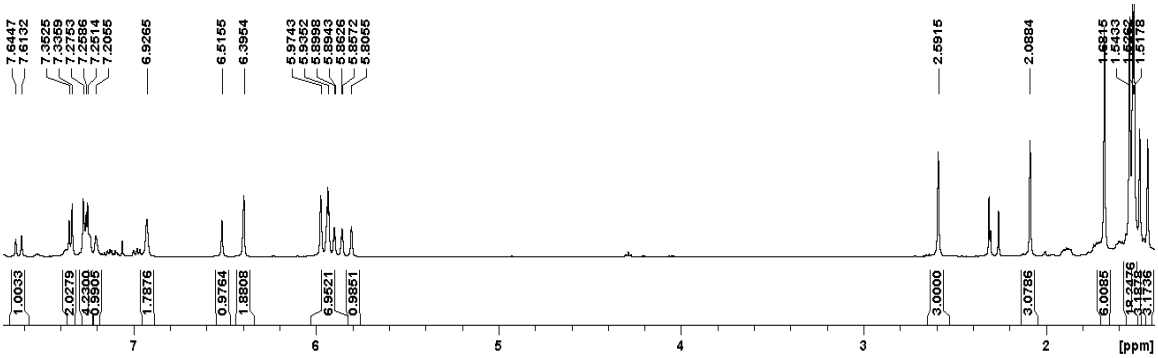

152.72, 155.66, 165.68. LCMS: 869 [M + Na] calculated, 869 found.

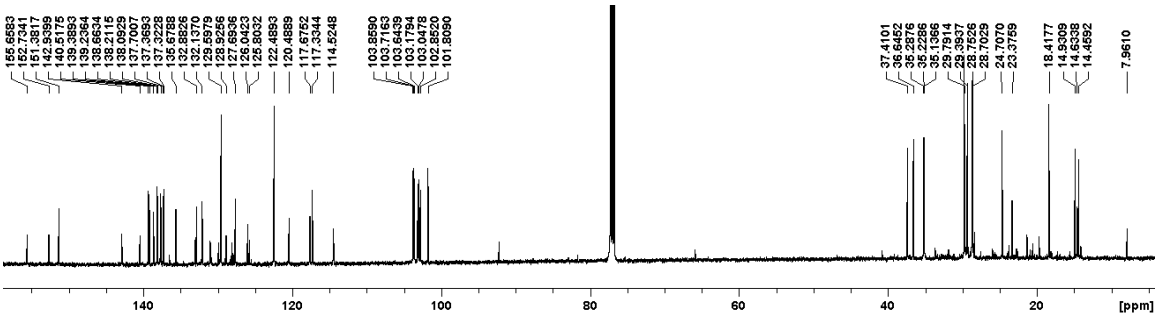

RAFT Copolymerization of 7 with MMA

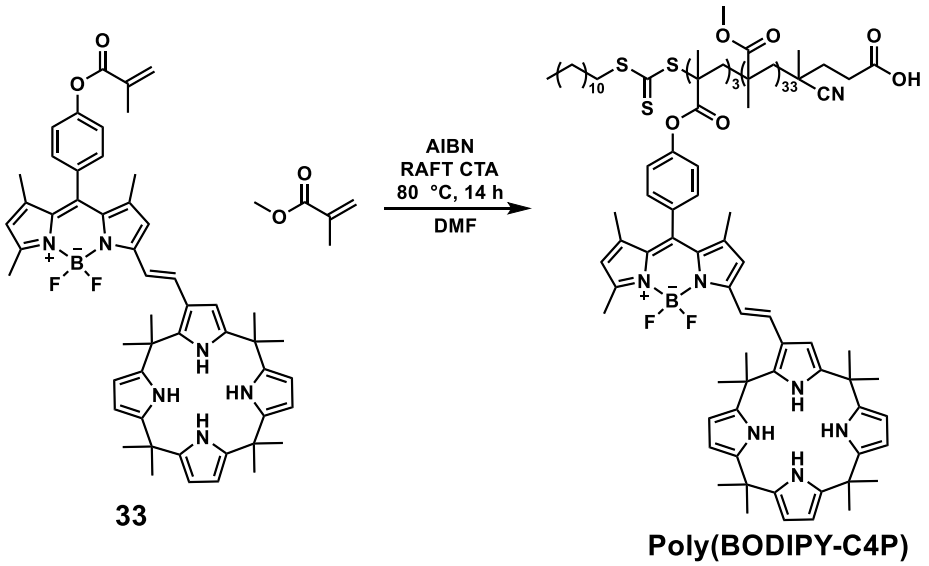

Compound **33** (33 mg, 0.03897 mmol), methyl methacrylate (0.077 mL, 0.74 mmol), AIBN (0.094 mg, 5.72 x 10^{-4} mmol), and 4-Cyano-4-[(dodecylsulfanylthiocarbonyl)sulfanyl]pentanoic acid (1.17 mg, 0.00289 mmol) were added using stock solutions and dissolved in 1.5 mL DMF. The reaction mixture was sparged with N_2 for 10 minutes and stirred for 14 hours at 80 °C. After 14 hours, the reaction mixture was placed into the freezer for 10 minutes. The polymer was then precipitated into diethyl ether, and centrifuged for 1 hour. The supernatant was removed and the purple solid was washed with diethyl ether 5 times to ensure removal of DMF. Removal of diethyl ether yielded **P1** as a purple solid (44 mg, 41 %) ^{1}H NMR (500 MHz, $CDCl_3$) δ (ppm) 0.83 (bs, 50 H), 1.01 (bs, 36 H), 1.41-1.53 (m, 40H), 1.67 (s, 8H), 1.80-1.94 (m, 53 H), 2.58 (s, 3H), 3.59 (bs, 99 H), 5.85-5.97 (m, 7H), 6.39 (s, 1H), 6.50 (s, 1H), 6.94 (bs, 2H), 7.20 (m, 3H), 7.33 (m, 4H), 7.62 (d, 1H). GPC: M_n = 16,670, M_w = 19,246, PDI = 1.15

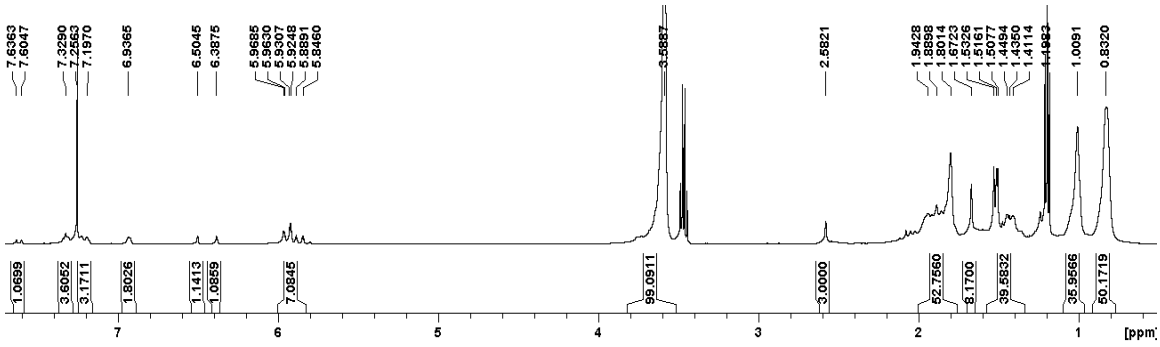
7.6363
7.6047
7.3290
7.2563
7.1970
6.9365
6.5045
6.3875
5.9685
5.9630
5.9307
5.9248
5.8981
5.8460
3.5887
2.5821
1.9428
1.8898
1.8014
1.6723
1.5326
1.5161
1.5077
1.4454
1.4350
1.4114
1.1983
1.0091
0.8320
1.0699
3.6052
3.1711
1.8026
1.1413
1.0859
7.0845
99.0911
3.0000
62.7560
8.1700
39.5832
35.9566
50.1719
7
6
5
4
3
2
1
[ppm]

References

1. Lehn, J M *Science* **1996**, *260*, 1762-1763
2. Amabilino, D. B.; Gale, P.A. *Chem. Soc. Rev.* **2017**, *46*, 2376-2377
3. Yudin, A. W. *Chem. Sci.* **2015**, *6*, 30-49
4. Kolesnichenko, I. V.; Anslyn, E. V. *Chem. Soc. Rev.* **2017**, *46*, 2385-2390
5. Albelda, M. T.; Frias, J. C.; Garcia-Espana, E.; Schneider, H. *Chem. Soc. Rev.* **2012**, *41*, 3859-3877
6. Nabeel, F.; Rasheed, T.; Bilal, M.; Li, C.; Yu, C.; Iqbal, H. M. N. *Sep. Purif. Rev.* **2020**, *49*, 20-36
7. Deng, H.; Wang, H.; Liang, M.; Su, X. *Microchem. J.* **2019**, *151*, 104250
8. Duan, Q.; Cao, Y.; Li, Y.; Hu, X.; Xiao, T.; Lin, C.; Pan, Y.; Wang, L. *J. Am. Chem. Soc.* **2013**, *28*, 10542-10549
9. Yoon, H.; Jang, W. *J. Mater. Chem.* **2010**, *20*, 211-222
10. Shcherbakova, E. G.; Zhang, B.; Gozem, S.; Minami, T.; Zavalij, P. Y.; Pushina, M.; Isaacs, L. D.; Anzenbacher, P. *J. Am. Chem. Soc.* **2017**, *139*, 14954-14960
11. Liu, Y.; Gill, A. D.; Duan, Y.; Perez, L.; Hooley, R. J.; Zhong, W. *Chem. Commun.* **2019**, *55*, 11563-11566
12. Biswakarma, D.; Dey, N.; Bhattacharya, S. (In Press). A Thermo-responsive Supramolecular Hydrogel that Senses Cholera Toxin via Color-Changing Response. https://pubs-rsc-org.ezaccess.libraries.psu.edu/en/content/articlepdf/2020/cc/d0cc00839g
13. Gao, W.; Zhang, H.; Jin, G. *Coord. Chem. Rev.* **2019**, *386*, 69-84
14. Syntrivanis, L.; Nemethova, I.; Schmid, D.; Levi, S.; Prescimone, A.; Bissegger, F.; Major, D. T.; Tiefenbacher, K. *J. Am. Chem. Soc.* **2020**, *142*, 5894-5900
15. Sinawang, G.; Osaki, M.; Takashima, Y.; Yamaguchi, H.; Harada, A. *Chem. Commun.* **2020**, *56*, 4381-4395
16. Cerny, J.; Hobza, P. *Phys. Chem. Chem. Phys.* **2007**, *9*, 5291-5303
17. Nishiyama, Y.; Langan, P.; Chanzy, H. *J. Am. Chem. Soc.* **2002**, *124*, 9074-9082
18. Cui, D.; Qian, X.; Liu, F.; Zhang, R. *Org. Lett.* **2004**, *6*, 2757-2760
19. Brak, K.; Jacobsen, E. N. *Angew. Chem. Int. Ed.* **2013**, *52*, 534-561
20. Banik, S. M.; Levina, A.; Hyde, A. M.; Jacobsen, E. N. *Science*, **2017**, *358*, 761-764
21. Chang, S. K.; Engen, D. V.; Fan, E.; Hamilton, A. D. *J. Am. Chem. Soc.* **1991**, *113*, 7640-7645
22. Pedersen, C. J. *Angew. Chem. Int. Ed.* **1988**, *27*, 1021-1027
23. Menon, S. K.; Hirpara, S. V.; Harikrishnan, U. *Rev. Anal. Chem.* **2004**, *23*, 233-267
24. Sokołowska, P.; Kowalski, M.; Jarosz, S. *Beilstein J. Org. Chem.* **2019**, *15*, 210-217
25. Kumar, R.; Sharma, A.; Singh, H.; Suating, P.; Kim, H. S.; Sunwoo, K.; Shim, I.; Gibb, B. C.; Kim, J. S. *Chem. Rev.* **2019**, *119*, 9657-9721.

26. Kim, H. J.; Kim, J. S. *Tetrahedron Lett.* **2006**, *47*, 7051−7055
27. Xue, M.; Yang, Y.; Chi, X.; Zhang, Z.; Huang, F. *Acc. Chem. Res.* **2012**, *45*, 1294-1308
28. Gale, P. A.; Sessler, J. L.; Kral, V. *Chem. Commun.* **1998**, 1-8
29. Davis, M. E.; Brewster, M. E. *Nat. Rev. Drug Discov.* **2004**, *3*, 1023-1035
30. Das, D.; Scherman, O. A. *Isr. J. Chem.* **2011**, *51*, 537-550
31. Kellersberger, K. A.; Anderson, J. D.; Ward, S. M.; Krakowiak, K. E.; Dearden, D. V. *J. Am. Chem. Soc.* **2001**, *123*, 11316-11317
32. Zheng, B.; Wang, F.; Dong, S.; Huang, F. *Chem. Soc. Rev.* **2012**, *41*, 1621-1636
33. Dong, S.; Luo, Y.; Yan, X.; Zheng, B.; Ding, X.; Yu, Y.; Ma, Z.; Zhao, Q.; Huang, F. *Angew. Chem. Int. Ed.* **2011**, *50*, 1905-1909
34. Nonokawa, R.; Yashima, E. *J. AM. CHEM. SOC.* **2003**, *125*, 1278-1283
35. Zhang, M.; Yang, Y.; Liu, L.; Chang, W.; Li, J. *Macromolecules* **2016**, *49*, 844−852
36. Blanda, M. T.; Adou, E. *Polymer* **1998**, *39*, 3821-3826
37. Harris, S. J.; Barrett, G.; McKervey, M. A. *J. Chem. Soc., Chem. Commun.* **1991**, 1224-1225
38. Crini, G. *Bioresour. Technol.* **2003**, *90*, 193-198
39. Badruddoza, A. Z. M.; Shawon, Z. B. Z.; Daniel, T. W. J.; Hidajat, K.; Uddin, M. S. *Carbohydr. Polym.* **2013**, *91*, 322-332
40. Alsbaiee, A.; Smith, B. J.; Xiao, L.; Ling, Y.; Helbling, D. E.; Dichtel, W. R. *Nature* **2016**, *529*, 190-194
41. Lange, R.F.; Van Gurp, M.; Meijer, E.W. *J. Polym. Sci. Pol. Chem.* **1999**, *37*, 3657-3670
42. Yanagisawa, Y.; Nan, Y.; Okuro, K.; Aida, T. *Science* **2018**, *359*, 72-76
43. Elacqua, E.; Geberth, G. T.; Bout, D. A. V.; Weck, M. *Chem. Sci.* **2019**, *10*, 2155-2152
44. Baeyer, A. *Ber. Dtsch. Chem. Ges*. **1886**, *19*, 2184
45. Gale, P. A.; Sessler, J. L.; Kral, V.; Lynch, V. *J. Am. Chem. Soc.* **1996**, *118*, 5140-5141
46. Gale, P. A.; Sessler, J. L.; Kral, V. *Chem. Commun.* **1998**, 1-8
47. Anzenbacher, P.; Try, A. C.; Miyaji, H.; Jursíková, K.; Lynch, V. M.; Marquez, M.; Sessler, J. L. *J. Am. Chem. Soc.* **2000**, *122*, 10268-10272
48. Warriner, C. N.; Gale, P. A.; Light, M. E.; Hursthouse, M. B. *Chem. Commun*. **2003**, 1810-1811
49. Miyaji, H.; Hong, S.; Jeong, S.; Yoon, D.; Na, H.; Hong, J.; Ham, S.; Sessler, J. L.; Lee, C. *Angew. Chem. Int. Ed*. **2007**, *46*, 2508–2511
50. Peng, S.; He, Q.; Vargas-Zúñiga, G. I.; Qin, L.; Hwang, I.; Kim, S. K.; Heo, N. J.; Lee, C.; Dutta, R.; Sessler, J. L. *Chem. Soc. Rev.* **2020**, *49*, 865-907
51. Sierra, A. F.; Hernandez-Alonso, D.; Romero, M. A.; Gonzalez-Delgado, J. A.; Pischel, U.; Ballester, P. *J. Am. Chem. Soc.* **2020**, *142*, 4276-4284

52. Miyaji, H.; Sato, W.; Sessler, J. L.; Lynch, V. M. *Tetrahedron Lett.* **2000**, *41*, 1369-1373
53. Anzenbacher, P.; Jursikova, K.; Sessler, J. L. *J. Am. Chem. Soc.* **2000**, *122*, 9350-9351
54. Miyaji, H.; Kim, H.; Sim, E.; Lee, C.; Cho, W.; Sessler, J. L.; Lee, C. *J. Am. Chem. Soc.* **2005**, *127*, 12510-12512
55. Taner, B.; Kursunlu, A. N.; Guler, E. *Spectrochim, Acta. A* **2014**, *118*, 903-907
56. Nishiyabu, R.; Anzenbahcer, P. *Org. Lett.* **2006**, *8*, 359-362
57. Miyaji, H.; Kim, H.; Sim, E.; Lee, C.; Cho, W.; Sessler, J. L.; Lee, C. *J. Am. Chem. Soc.* **2005**, *127*, 12510-12512
58. Ghorpade, T. K.; Patri, M.; Mishra, S. P. *Sens. Actuat. B Chem.* **2016**, *225*, 428-435
59. Iv, Y.; Xu, J.; Guo, Y.; Shao, S. *J Incl Phenom Macro* **2012**, *72*, 95–101
60. Gotor, R.; Costero, A. M.; Gavina, P.; Gil, S.; Parra, M. *Eur. J. Org. Chem.* **2013**, 1515–1520
61. Lite, P. F.; Aniceto, J. P. S.; Silva, C. M. *Water Air Soil Pollut.* **2012**, *223*, 6133-6155
62. Handy, S. T., Bregman, H., Lewis, J., Zhang, X., & Zhang, Y. *Tetrahedron Lett.* **2003**, *44*, 427-430
63. Jedinák, L., Zátopková, R., Zemánková, H., Šustková, A., & Cankař, P. *J. Org. Chem.* **2017**, *82*, 157-169
64. Silver, E. S.; Rambo, B. M.; Bielawski, C. W.; Sessler, J. L. *J. Am. Chem. Soc.* **2014**, *136*, 2252-2255
65. Carrow, B. P.; Hartwig, J. F. *J. Am. Chem. Soc.* **2011**, *133*, 2116-2119
66. Aydogan, A.; Coady, D. J.; Lynch, V. M.; Akar, A.; Marquez, M.; Bielawski, C. W.; Sessler, J. L. *Chem. Commun.* **2008**, 1455-1457
67. Aydogan, A.; Coady, D. J.; Kim, S. K.; Akar, A.; Bielawski, C. W.; Marquez, M.; Sessler, J. L. *Angew. Chem. Int. Ed.* **2008**, *47*, 9648 –9652
68. Aydogan, A. *Supramol. Chem*. **2016**, *28*, 117-124
69. Ji, X.; Guo, C.; Ke, X.; Chi, X.; Sessler, J. L. *Chem. Commun*. **2017**, *53*, 8774-8777
70. Ji, X.; Guo, C.; Chen, W.; Long, L.; Zhang, G.; Khashab, N. M.; Sessler, J. L. *Chem. Eur. J.* **2018**, *24*, 15791-15795
71. Patil, N. G.; Basutkar, N. B.; Ambade, A. V. *Chem. Commun*., **2015**, *51*, 17708-1771
72. Jiang, Z.; Wang, Y. *Chem. Lett.*, **2003**, *32*, 568-569
73. Kollmannsberger, M.; Rurack, K.; Resch-Genger, U.; Daub, J. *J. Phys. Chem. A*, **1998**, *102*, 10211-10220
74. Rurack, K.; Kollmannsberger, M.; Resch-Genger, U.; Daub, J. *J. Am. Chem. Soc.*, **2000**, *122*, 968-969
75. http://supramolecular.org

76. D. B. Hibbert and P. Thordarson, *Chem. Commun*. **2016**, *52*, 12792-12805
77. Siro, I.; Plackett, D. *Cellulose* **2010**, *17*, 459-494
78. Loerbroks, C.; Rinaldi, R.; Thiel, W. *Chem. Eur. J.* **2013**, *19*, 16282-16294
79. Csoka, L.; Hoeger, I. C.; Rojas, O. J.; Peszlen, I.; Pawlak, J. J.; Peralt, P. N. *ACS Macro Lett.* **2012**, *1*, 867-870
80. Chae, I.; Jeong, C. K.; Ounaies, Z.; Kim, S. H. *ACS Appl. Bio Mater.* **2018**, *1*, 936-953
81. French A. D. *Cellulose* **2014**, *21*, 885-896
82. Wada, M.; Nishiyama, Y.; Langan, P. *Macromolecules* **2006**, *39*, 2947-2952
83. Wada, M.; Kwon, G. J.; Nishiyama, Y. *Biomacromolecules* **2008**, *9*, 2898-2904
84. Chanzy, H.; Henrissat, B.; Vincendon, M.; Tanner, S. F.; Belton, P. S. *Carbohydr. Res.* **1987**, *160*, 1-11
85. Roche, E.; Chanzy, H. *Int. J. Biol. Macromol.* **1981**, *3*, 201-206
86. Lee, C. M.; Mittal, A.; Barnette, A. L.; Kafle, K.; Park, Y. B.; Shin, H.; Johnson, D. K.; Park, S. Kim, S. H. *Cellulose* **2013**, *20*, 991-1000
87. Gong, J.; Mo, L.; Li, J. *Carbohydr. Polym.* **2018**, *195*, 18-28
88. De France, K. J.; Yager, K. G.; Hoare, T.; Cranston, E. D. *Langmuir* **2016**, *32*, 756407571
89. Habibi, Y.; Heim, T.; Douillard, R. *J. Polym. Sci. Polym. Phys.* **2008**, *46*, 1430-1436